Journal Pre-proofs

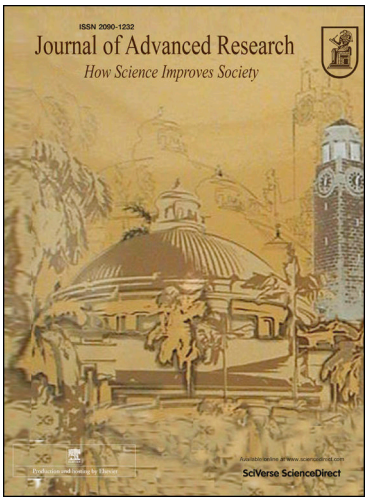

Akkermansia muciniphila-derived postbiotics reprogram immune balance to combat sepsis via the IDO1/Kyn/AhR metabolic axis

Yuting Zhang, Ruopeng Yin, Wang Dong, Li Sun, Tao Wang, Jingzu Sun, Huanqin Dai, Yanliang Bi, Liangliang Wang, Hongwei Liu

PII: S2090-1232(26)00528-X
DOI: https://doi.org/10.1016/j.jare.2026.07.010
Reference: JARE 3067

To appear in: *Journal of Advanced Research*

Received Date: 15 February 2026
Revised Date: 31 May 2026
Accepted Date: 2 July 2026

Please cite this article as: Zhang, Y., Yin, R., Dong, W., Sun, L., Wang, T., Sun, J., Dai, H., Bi, Y., Wang, L., Liu, H., *Akkermansia muciniphila*-derived postbiotics reprogram immune balance to combat sepsis via the IDO1/Kyn/AhR metabolic axis, *Journal of Advanced Research* (2026), doi: https://doi.org/10.1016/j.jare.2026.07.010

Akkermansia muciniphila-derived postbiotics reprogram immune balance to combat sepsis via the IDO1/Kyn/AhR metabolic axis

Yuting Zhang[1,2,3#], Ruopeng Yin[1,2,3#], Wang Dong[1,2,3], Li Sun[1,2,3], Tao Wang[1,3], Jingzu Sun[1,3], Huanqin Dai[1,2,3], Yanliang Bi[4], Liangliang Wang[1,3], Hongwei Liu[1,2,3]*.

[1] State Key Laboratory of Microbial Diversity and Innovative Utilization, Institute of Microbiology, Chinese Academy of Sciences, Beijing, P. R. China.

[2] Medical School, University of Chinese Academy of Sciences, Beijing, P. R. China.

[3] The Laboratory of Microbiome and Microecological Technology, Institute of Microbiology, Chinese Academy of Sciences, Beijing, P. R. China.

[4] Key Laboratory of Feed Biotechnology of the Ministry of Agriculture and Rural Affairs, Institute of Feed Research of Chinese Academy of Agricultural Sciences, Beijing 100193, China.

[#] These authors contributed equally: Yuting Zhang, Ruopeng Yin.

* Corresponding: liuhw@im.ac.cn (Hongwei Liu). Email: liuhw@im.ac.cn

CRediT author statement

Yuting Zhang: Conceptualization, Methodology, Writing-Original Draft. **Ruopeng Yin**: Data Curation, Supervision. **Wang Dong**: Methodology. **Li Sun**: Conceptualization. **Tao Wang**: Formal analysis. **Jingzu Sun**: Resources. **Huanqin Dai**: Resources. **Yanliang Bi**: Resources. **Liangliang Wang**: Supervision, Data Curation. **Hongwei Liu**: Data Curation, Resources, Conceptualization.

Acknowledgments

This work was financially supported by the National Natural Science Foundation of China (92578117) and the National Key Research and Development Program of China (2022YFA1304200).

Abstract

Introduction: Sepsis is a life-threatening syndrome of organ dysfunction driven by a dysregulated immune response. Effective therapeutic strategies to restore immune homeostasis remain limited. Hypoacylated lipooligosaccharides (ALOS) from *Akkermansia muciniphila* have emerged as potential immunomodulatory postbiotics, yet their therapeutic potential in sepsis and the underlying mechanisms remain unexplored.

Objectives: This study aims to investigate whether ALOS confers protection in experimental models of sepsis induced by toxic lipopolysaccharides (LPS) or cecal ligation and puncture (CLP), and the mechanism by which ALOS exerts its anti-inflammatory and regulatory effects.

Methods: In LPS or CLP-induced mouse sepsis models and a porcine sepsis model, ALOS (0.2 mg/kg, i.p.) was administered once every two days before challenge or half an hour post-surgery. Survival rates, physiological and biochemical parameters were assessed. Based on 16S rRNA gene amplicon sequencing and barrier function assessment, the changes of the colonic microbiota and metabolites and anti-inflammatory capacity were analyzed. The anti-inflammatory and immunomodulatory mechanisms of ALOS were investigated through dendritic cell phenotyping, transcriptomic analysis, inhibitor assays, and conditioned medium experiments. Finally, the safety of ALOS was evaluated in C57BL/6J mice following one-week administration (0.2 mg/kg, i.p.).

Results: ALOS pretreatment significantly suppresses sepsis, reduces the proportion of pro-inflammatory Th17 cells, and increases regulatory T cells (Treg). Mechanistically, ALOS induced semi-mature dendritic cells with upregulated IDO1 expression, leading to enhanced production of kynurenine (Kyn). Kyn activated the aryl hydrocarbon receptor (AhR) to drive Treg differentiation. The protective effect of ALOS was completely reversed by NLG919, whereas Kyn administration mimicked the therapeutic benefit. ALOS also produced therapeutic protection on sepsis. In a porcine sepsis model, pretreatment of ALOS exerted systemic anti-inflammatory effects and protected multiple organs.

Conclusion: This study highlights the protective role of ALOS in sepsis and identifies the IDO1-Kyn-AhR immune axis as the major underlying mechanism.

Keywords: *Akkermansia muciniphila*, lipooligosaccharides, sepsis, semi-mature

dendritic cells, Treg cells, IDO1-Kyn-AhR.

Introduction

Sepsis is a complex condition characterized by dysregulated immune responses to pathogen-associated infection, which is intricately associated with acute organ dysfunction and exhibits a high incidence rate.[1, 2] At the onset of sepsis, pathogen triggers immune cells to enter a heightened inflammatory state, culminating in a cytokine storm.[3, 4] While initially beneficial for pathogen control, this response subsequently causes significant damage to the immune system and vulnerable organs.[5] Suppressing the early uncontrolled inflammatory response and preventing multiorgan damage represent key strategies for reducing acute sepsis mortality. Moreover, the hyperinflammation response is often followed by a compensatory immunosuppressive state, further challenging clinical management. Current sepsis management (source control, antibiotics, resuscitation, organ support) yields limited outcomes due to significant difference in individual immune responses.[6] Newly developed drugs such as anti-TNF-α/IL-1β biologics, TLR4 antagonists, immune checkpoint inhibitors, and mesenchymal stem cells showed limited clinical efficacy and lower safety in trials,[7, 8] underscoring the urgent need for alternative immunomodulatory strategies.

In recent works on inflammatory diseases, postbiotics produced by gut probiotics have been reported to exert antimicrobial, immunomodulatory, antioxidant, and gut barrier-reinforcing effects, offering a promising complementary approach. Their superior stability, safety, and suitability for standardized manufacturing confer substantial advantages over live probiotics in applications. Among postbiotics, hypo-acylated lipopolysaccharides (LPS) from Gram-negative gut bacteria, have recently attracted considerable attention due to their potent immunomodulatory activities.[9-11] For example, LPS of *Bacteroides vulgatus* induce semi-mature $CD11c^{+}$ cells and downregulates the pathogenic Th17 cells in T cell transfer model of chronic colitis.[12] *B. fragilis*-derived tetra-acylated and monophosphorylated lipid A moiety of LPS promote colonic $ROR\gamma t^{+}$ Treg cells by inducing sustained IFN-β production in dendritic cells (DCs), while concurrently suppressing Th17 cell responses in the colitis model.[13] *Parabacteroides goldsteinii* lipopolysaccharide is anti-inflammatory, and significantly ameliorates chronic obstructive pulmonary disease (COPD) by acting as an antagonist of TLR4 signaling pathway.[14] In the field of sepsis treatment, penta-acylated LPS from *Bartonella quintana* improve the survival rate in LPS/D-galactosamine-induced lethal mouse endotoxaemia.[15] Eritoran, a synthetic analogue of the penta-acylated lipid A moiety of LPS from *Rhodobacter sphaeroides*, suppresses endotoxin-induced cytokine production and was the first TLR4 antagonist to enter a phase III clinical trial for severe sepsis.[16] However, the precise molecular mechanisms underpinning the therapeutic effects of these LPS molecules have yet to be fully elucidated.

The disrupted gut microbiota leads to dysregulation of gut mucosal immune, thereby predisposing to infection.[17] In septic patients, the probiotic bacterium *Akkermansia muciniphila* is significantly reduced compared to healthy individuals, and pretreatment with this probiotic confers protection against sepsis in animal models.[18, 19] Recently,

a variety of postbiotics have been reported from *A. muciniphila*. For instance, the peptide RKH exerts inhibitory binding to TLR4 signal transduction in immune cells, thereby attenuating sepsis-induced systemic inflammation.[18] The Amuc_1100 blunted the sepsis-induced acute lung injury by modulating of gut microbiota.[20] Harmaline inhibits p65 activation and suppresses virus-induced systemic inflammation.[21] In previous study, we identified LPS from *A. muciniphila* (ALPS), which is structurally characterized with tetra-acylated lipid A species and unique oligosaccharide chains (Fig. S1A), and demonstrated its anti-obesity efficacy through activation of the TLR4-IL-22 pathway.[22, 23] Schneider have introduced the term "lipooligosaccharides" (LOS) to describe a class of lipopolysaccharides (LPS) that lack O-antigen chains and possess relatively short carbohydrate moieties.[24] To more precisely reveal the chemical nature of ALPS, we re-defined the ALPS as *A. muciniphila* LOS (ALOS) in this work. Building on their unique immune activity, we hypothesize that ALOS may contributes to its protective effects against sepsis.

In this work, we demonstrate that ALOS confers protection in both murine and porcine models of sepsis by activating the IDO1-kynurenine-AhR axis in dendritic cells, and subsequently promoting Treg differentiation and ILC3-derived IL-22 to restore tissue homeostasis. Our findings present ALOS as a novel therapeutic approach to treat sepsis.

Materials and methods

Extraction of LOS from *A. muciniphila*

A. muciniphila HW07 stored in China General Microbiological Collection Center (CGMCC) with the accession number of 40794 was cultured at 37°C for 5 days in anaerobic modified brain heart infusion (BHI) broth (BD Biosciences; 237500) with supplementation of mucin under an atmosphere of 10% H_2, 10% CO_2 and 80% N_2 (AW500SG anaerobic workstations; ELECTROTEK, England). The LOS of *A. muciniphila* were extracted and purified according to our early reported method.[22] The nature of ALOS was analyzed by SDS-PAGE and silver staining. The composition and distribution of oligosaccharides and fatty acids in ALOS have been clarified by two previous investigations. [22, 23] Note on nomenclature: The LOS extracted from *A. muciniphila* HW07 and investigated in this study are identical to the molecule previously designated as ALPS (*A. muciniphila*-derived LPS) in our earlier report.[22] Given the confirmed absence of an O-antigen repeating unit, a feature that formally classifies this molecule as a LOS rather than a smooth-type LPS, we have adopted the term ALOS throughout this manuscript to more accurately reflect its structural characteristics.

Bone marrow cells culture and assays

Bone marrow cells were isolated from the tibia and femur of C57BL/6J WT mice (6-10 weeks old) and cultivated by methods previously described.[22] BM cells (2.0×10^4)

were seeded in 10 cm non-treated cell culture dishes and cultured for 9 days in the presence of murine GM-CSF (20 ng/mL, Med-Chem-Express; HY-P7361) and IL-4 (1 ng/mL, Novoprotein; CK15) in RPMI-1640 (Dakewe; 6016011) with Penicillin-Streptomycin-Amphotericin B Solution (IMMOCELL; IMC-602) for BM-derived dendritic cell (BMDC) differentiation. For antagonism assay, BMDCs were pre-treated with ALOS (25 or 100 ng/mL) for 12 h/6 h and then stimulated with *E. coli* LPS (100 ng/mL) for 6 h. Cell culture dishes/plates and centrifuge tubes were obtained from NEST Biotechnology Co. Ltd. (Wuxi, China).

For acute transient transfection, cells were seeded one day prior to transfection. The HighGene Transfection Reagent/siRNA complex (Abclonal; RM09014) was prepared according to the manufacturer's protocol. Cells were incubated with the complex for 24 to 48 hours.

Animal assay for sepsis

Six- to eight-week-old male of C57BL/6J mice were purchased from GemPharmatech Co., Ltd. Tlr4−/− mice (Cyagen Biosciences) were used for breeding. All animals were kept and bred under specific pathogen-free (SPF) conditions in individually ventilated cages (IVCs), receiving standard chow and regular drinking water. All animal experiments were performed in strict accordance with the Laboratory Animal Management Regulations of China. The experiments were conducted following the guidelines for Laboratory Animal Care and were approved by the Laboratory Animal Welfare and the Ethics Committee of Institute of Microbiology (IMCAS2022046), Chinese Academy of Sciences.

The Cecal ligation and puncture (CLP) operation was conducted following established protocols from the literature.[18] Briefly, mice were deeply anesthetized, and a 2cm midline laparotomy was performed under aseptic conditions to expose the cecum. The distal half of the cecum was ligated and then punctured once through-and-through with an 18gauge needle, allowing a small amount of fecal matter to extrude. The cecum was returned to the abdominal cavity, and the peritoneum was closed. Finally, mice were resuscitated by subcutaneous administration of 1 mL sterile saline (Uprise; aprslhn). Mice in the sham operation group underwent laparotomy and suture operation without ligature and puncture. Mice with LPS-induced lethal endotoxemia were intraperitoneally injected with *E. coli* O111: B4 LPS (15 mg/kg, Sigma; 437627). The LPS-induced endotoxemia and CLP models are complementary: LPS provides a chemically defined, highly reproducible system for pharmacological analysis, whereas CLP better recapitulates the clinical complexity of polymicrobial peritonitis in a physiologically relevant infectious setting.

To investigate the protective role of ALOS in septic mice, mice were subjected to sepsis induced by CLP or LPS treatment and pretreated with intraperitoneal ALOS (0.2 mg/kg) once every two days before challenge (n=18 per group), a dosing regimen adopted with slight modification from previous studies.[22, 25] Mouse survival was

monitored 72 hours after CLP surgery or LPS injection. Mice were euthanized12 hours after CLP surgery or LPS injection to assess systemic inflammation and organ damage indices.

For pseudo-germ-free septic mice, mice were given with a broad- spectrum antibiotic cocktail (Ampicillin (1 g/L) (Macklin; 69-53-4), Metronidazole (0.5 g/L) (YUANYE; S17079), Neomycin (0.5 g/L) (Meryer; 1405-10-3), Vancomycin (0.5 g/L) (Aladdin; 1404-93-9)) in drinking water for 7 consecutive days. After establishing the pseudo-germ--free mice, ALOS or vehicle was administrated intraperitoneally every two days (n=18 per group). Mice were intraperitoneally challenged with toxic *E. coli* LPS to induce sepsis. Survival was monitored over time.

For IDO1 antagonizing experiments, mice were pretreated with NLG919 (100 mg/kg/day, i.g.) (MeilunBio; MB5145) for 12 days (n=14 per group). The effective inhibition of IDO1 was confirmed by assessing Ido1 expression levels in sampled tissues. ALOS (0.2 mg/kg) was administered intraperitoneally (i.p.) once in two days prior to toxic LPS (15 mg/kg) i.p. administration.

For the experiment of the kynurenine (Kyn) supplementation, mice were intraperitoneally pretreated with Kyn (TargetMol; 2922-83-0, 5 mg/kg) daily for 8 days (n=14 per group) and were intraperitoneally treated with toxic LPS (*E. coli* LPS) (15 mg/kg) on the eighth day.

For the therapeutic experiments of ALOS, sepsis was induced by CLP. Half an hour after surgery, mice received an intraperitoneal injection of ALOS (0.2 mg/kg) or vehicle. Survival was monitored over a defined period. For endpoint analyses, a separate cohort of mice (n = 8 per group) was euthanized 12 h post-surgery; blood and tissues were collected for further assessment.

For piglet sepsis assay, male newborn Bama pigs (body weight range 2.5-3.8 kg) were housed under standard conditions with free access to feed and water. Bama piglets were randomly assigned to two groups: ALOS pretreatment group (n = 4, 4 μg/kg, i.p., once every two days for four days prior to LPS challenge) and vehicle control group (n = 4). The porcine sepsis model was established via intraperitoneal injection of LPS (200 μg/kg). Blood samples were collected via jugular venipuncture into EDTA-containing tubes at predefined time points after LPS challenge, and tissue samples (heart, lung, liver, kidney) were harvested immediately after euthanasia and fixed in 4% ploy-formaldehyde (PFA) (Biotopped; Top0382) for histopathological analysis. Piglets model experiments were performed in accordance with the Laboratory Animal Management Regulations of China. The experiments were conducted following the guidelines for Laboratory Animal Care and were approved by the Laboratory Animal Welfare and the Ethics Committee of Experimental Animals, Feed Research Institute, Chinese Academy of Agricultural Sciences, approved all procedures used in this experiment (approval number: IFR-CAAS-20220518)

Cytokine analysis by ELISA

Cell culture supernatant was obtained by centrifugation at 1800 rpm for 5 min to remove debris. Mouse blood was collected into EDTA containing tubes, allowed to clot for 4 h at room temperature, and centrifuged at 12,000 rpm for 1 min. Porcine blood was collected in tubes containing EDTA (Biotopped; Top9181S) after venipuncture and centrifuged at 3,000 rpm for 10 min at 4 °C.

The cytokine concentrations of mouse TNF-α (Proteintech; KE10002), IL-6 (Solarbio; SEKM-0007), IL-22 (E-MSEL-M0040; Elabscience), and IL-1β (Jiangsu Meimian Industrial Co., Ltd; MM-0040M1) were determined using commercially available ELISA kits, following the manufacturer's instructions. TNF-α, IL-6, and IL-1β are core drivers of the cytokine storm and organ dysfunction in both murine and porcine sepsis models. Mouse Kyn level was quantified using an ELISA kit (Dogesce; DG30820M-48) following the manufacturer's instructions. The pig TNF-α (Abebio; AE13960PI), IL-6 (Abebio; AE38207PI), and C-reactive protein (a biomarker of systemic inflammation) (G-CLONE; SEK-03001368) levels were quantified using ELISA kits following the manufacturer's instructions. The centrifuge tubes used in all the above experiments were purchased from Crystalgen, HefeiKejing Biotechnology Co.Ltd.

Biochemical analysis

The levels of plasma or serum γ-glutamyl transpeptidase (Abbkine; KTB1690), Urea (Mreda; M052961), creatinine (Sangon Biotech; D799853-0096), Creatine Kinase (Geruisi; G0855W96), alanine transaminase (ALT) (Njjcbio; C009-2-1) and aspartate transaminase (AST) (Njjcbio; C010-2-1) levels were determined with commercially available kits according to the manufacturers' instructions.

Histopathological examination

The heart, lung, liver and kidney tissues from mice and piglets were collected and fixed with 4% paraformaldehyde (PFA) phosphate buffered saline (pH 7.4) for 36 h. The paraffin-embedded samples were sliced and stained with hematoxylin/eosin (H&E) staining kit. The slices were observed under a microscope.

For immunohistochemistry, paraffin-embedded tissue sections were stained with anti-Notch1 antibody (1:100), anti-β-catenin antibody (1:100), anti-Lgr5 antibody (1:100), and visualized by 3,3'-Diaminobenzidine (DAB) staining according to manufacturer's instructions. For immunofluorescence, paraffin-embedded tissues were stained with anti-IL-22 antibody (1:100). The slides were independently assessed by two researchers blinded to the sample identities.

Real-time qPCR (RT-qPCR) assays

Total RNA was isolated from tissue and cell samples using Trizol reagent (YEASEN; 10606ES60) and isopropanol (J&K; 67-63-0), and then dissolved in deionized water (SL2240; Coolaber). Subsequently, RNA was reverse-transcribed into complementary DNA (cDNA) following the instructions of a commercial reverse transcription kit

(YEASEN; 11151ES60). RNasin (Glycerol-Free) was purchased from ATG Biotechnology Co., Ltd, Nanjing, China. Gene expression was then analyzed by RT-qPCR, β-actin was used as control and gene relative expression was calculated using the $2^{-\Delta\Delta Ct}$ method. All primers for RT-qPCR were listed in Supplemental Table.

RNA-sequencing of BMDC

RNA was extracted from BMDCs treated with or without ALOS using Trizol reagent (Abclonal; RK30129), and library construction was performed using a SMART-seq2 protocol. Sequencing libraries were sequenced on an DNBSEQ T7 (PE150) by Novogene. Sequencing reads were aligned to the mouse transcriptome (GRCm38 ensembl v101; cDNA and ncRNA) and quantified. The expression of transcript was calculated in RPKM (reads per kilobase per million). All differentially expressed genes were plotted with the "heatmap" and "ggplot2" R packages. For KEGG enrichment analysis, p-value <0.05 was used as a threshold to determine significant enrichment for gene sets with the "clusterProfiler" R package.

Conditioned medium assay

BMDCs were treated with 100 ng/mL of ALOS for 12 hours. After removing the culture medium, cells were washed three times with ice-cold PBS (Cas9X/HyCyte, Haixing Biosciences, GUPB-R001) and then replenished with fresh RPMI medium (VivaCell, Shanghai, China; C3010-0500) for an additional 12-hour culture. The culture supernatant was collected and filtered through a 0.22 μm filter to generate conditioned medium (BMDC-CM). The excised spleen was dissected from C57BL/6J mice and mechanically dissociated through a 40 μm cell strainer using the plunger of syringe. After red blood cell digestion with RBC Lysis Buffer (CWBIO, China; CW0613S), Naïve $CD4^+$ T cells were extracted using the EasySepTM Mouse Naïve CD4+T Cell Isolation Kit (STEMCELL; 19765). Naïve T cells were stimulated and expanded using CD3/CD28 T cell activation/enhancement magnetic beads (Abclonal, RK50024) for 5 days, followed by addition of 5 ng/mL of TGF-β (TargetMol; TMPY-00608) and 100 U/mL of IL-2 (ABclonal; RP01384) to serum-containing DMEM medium (Dakewe; 6016121), affording Naïve Treg cells. The obtained iTreg cells were then cultured with the BMDC-CM. Subsequently, the iTreg cells were analyzed by flow cytometry and immunofluorescence and compared with the positive control supplemented with 50 μM Kyn (TargetMol; T4928).

Co-culturing of ALOS-treated BMDCs with iTreg cells

ALOS-BMDCs and iTreg cells were generated as above described. ALOS-BMDCs (2×10^4) or blank BMDCs (control) were co-cultured with 2×10^5 iTreg cells (ratio 1:10) in 200 μL RPMI 1640 with 10% FBS in 96-well plates. After 12 h incubation, cells were harvested and Flow cytometry was performed to quantify MHC-II^+ DC and $Foxp3^+CD25^+$ Treg cells.

Immunofluorescence staining

Fresh intestinal tissues were fixed in 4% paraformaldehyde (PFA) for 24 h, cryoprotected, embedded, and cut into 3–5 μm sections. The sections were blocked with 5% bovine serum albumin (BSA)(YUANYE; S12012) for 30 min, and then incubated overnight at 4°C with rabbit anti-IL-22 polyclonal antibody (Zenbio; R30198). After washing, the sections were stained with goat anti-rabbit IgG-Cy3 for 50 min at room temperature. For BMDCs, cells seeded on a glass plate were treated with 1 μg/mL ALOS for 7 h, washed with cold PBS after removing supernatant, and then fixed in 4% PFA for 1h at room temperature. The cells were treated with cell penetrating solution (Beyotime; P0096) for 1h. Cells were washed twice with cold PBS (pH 7.4) (New Cell & Molecular Biotech; C500C1), then incubated with anti-AhR (Bioss; bs-1416R), anti-β-Tubulin (Beyotime; AF2835) overnight at 4°C. After washing with 1mL PBST buffer (0.1% tween-80; pH 7.4), cells were incubated with DyLight 488 goat anti-mouse IgG (Abbkine; A23210) or DyLight 549 goat anti-rabbit IgG (Abbkine; A23320) diluted with 5% goat serum for another 1 h at room temperature in the dark. Treg cells were treated with ALOS-BMDC-CM and subsequently stained according to the kit protocol. Fluorescence was visualized under a Leica SP8 confocal microscope.

Flow cytometry analysis for immune cells

Single-cell suspensions of tissue or lymph nodes were prepared as described.18 Briefly, Spleens and mesenteric lymph nodes (MLNs) were harvested and processed into single-cell suspensions by mechanical dissociation through a 70 μm strainer in ice-cold FACS buffer (PBS + 2% FBS (Royacel; RY-F81-05)). Erythrocytes in spleens were lysed by ACK buffer prior to washing and counting. For intestinal lamina propria cell isolation, intestinal tissues were cleared of Peyer's patches, cut into segments, and treated with PBS (Mei5Bio, Beijing, China; MF224-01,) supplemented with DTT and EDTA (containing 1 mM DTT (Dogesce, BG295) and 5 mM EDTA (Biotopped, Top9181S)) under shaking at 37°C for 20-30 min to deplete epithelial cells. The obtained lamina propria tissue was washed and subjected to enzymatic digestion in collagenase/DNase I-containing medium (1 mg/ml type IV collagenase and 20 μg/ml DNase I (ZOMANBIO; H171)) with shaking at 37°C for two or three rounds (20-30 min each). For each round, the supernatant was collected and the enzyme activity was neutralized with FACS buffer. The supernatants were combined, filtered through a 70 μm cell strainer (Bioland; CS05-070B), and centrifuged at 700 g for 5 min to obtain lamina propria cell pellets. For in vitro cell assay, harvested cells were washed twice with PBS. Mouse peripheral blood lymphocytes were isolated using the Mouse Peripheral Blood Lymphocyte Isolation Solution Kit (Solarbio, P8620).

The single-cell suspensions prepared above were Fc-blocked (anti-CD16/32, 10 min) (14-9161-73, ThermoFisher), then stained with surface specific antibody for 20-30 min at room temperature in the dark). Cells were washed with buffer, fixed, and permeabilized using a commercial transcription factor staining kit. Intracellular staining was performed with antibodies for 30-60 min. For flow-cytometry analysis, cells were resuspended in FACS Buffer.

Western blot analysis

BMDCs were lysed using cell lysis buffer (Innochem; B2243). Nuclear and cytoplasmic proteins were then extracted separately using a commercial subcellular protein fractionation kit (CWBIO; CW0199S). Protein concentrations were quantified using BCA protein assay kit. The protein samples were mixed with SDS-PAGE loading buffer (ABclonal; RM00001) and denatured by heating. Proteins were separated on 4-20% SDS polyacrylamide gels (TSINGKE; TSP024-12) and then transferred to 0.22 μm PVDF membranes (Yeasen; 36125ES03). Membranes were blocked with 5% Skimmed milk (RM00014, Abclonal) for 15 minutes, and then blocked with primary antibodies (AhR, Bioss; bs-1416R) (CYP1A1, Promabio; P07237; ProMab Biotechnologies Inc.) at 4°C overnight. The membranes were then incubated with secondary antibody-conjugated HRP (1:10000, Abcam) for 1 hour at room temperature, and bands were visualized using an ECL kit (FD8000, Fdbio science, China). β-actin served as a cytoplasmic loading control. Histone 3 served as a nuclear loading control.

Gut microbiota analysis

Caecal content DNA was extracted using a standardized protocol. The extracted DNA was quantified, assessed for purity, and subjected to PCR amplification targeting the V3-V4 hypervariable region of the 16S rRNA gene. The primer pair used was 338F (5′-ACTCCTACGGGAGGCAGCA-3′) and 806R (5′-GGACTACHVGGGTWTCTAAT-3′). Amplified products were purified, normalized, and sequenced on the Illumina NovaSeq platform using a paired-end strategy (2 × 300 bp). Raw sequencing reads were quality-filtered, denoised, and clustered into amplicon sequence variants (ASVs) following the bioinformatics pipeline.

Statistical analysis

Statistical analyses were conducted using Graph Pad Prism 9.5.2 (CA, USA). Data normality was first assessed with the Shapiro–Wilk test. For normally distributed data, comparisons between two groups were analyzed with a two-tailed Student's t-test, while comparisons among three or more groups used one-way ANOVA followed by Tukey's post hoc test. For non-normally distributed data, nonparametric tests were applied: the Mann–Whitney U test for two-group comparisons and the Kruskal–Wallis test with Dunn's post hoc analysis for groups of three or more. The Mantel- Cox log-rank test was used to compare the survival curves. Statistical significance was set at $p \leq 0.05$.

Data availability statement

RNA-seq data reported in this paper have been deposited in the NCBI Sequence Read Archive (SRA) and can be accessed through BioProject ID: PRJNA1393444 (https://www.ncbi.nlm.nih.gov/sra/PRJNA1393444). 16S RNA sequencing data have been deposited in the NCBI's SRA and can be accessed through BioProject ID:

PRJNA1414504. Supporting Information (figures, tables, graphical abstract) may be found online.

Result

ALOS modulates dendritic cell responses to toxic LPS

In an early work, ALOS was demonstrated to alleviate diet-induced metabolic endotoxemia and reduce inflammatory response in obese mice.[22] This prompted us to explore whether treatment with ALOS prevent the inflammation triggered by toxic LPS (Fig. S1B). We found that co-treatment of bone marrow-derived dendritic cells (BMDCs) with ALOS and *E. coli* toxic LPS significantly enhanced the secretion of TNF-α (Fig. S1C). By contrast, BMDCs primed by ALOS showed hypo-response to subsequent *E. coli* toxic LPS stimulation, as evidenced by reduced TNF-α secretion in comparison with the non-primed cells (Fig. S1D-E).

ALOS confers protection in murine models of sepsis

Given the pivotal role of endotoxin in septic shock,[26] we next assessed the protective effect of ALOS on toxic LPS-induced endotoxemia *in vivo*. Mice were first treated with ALOS in different dosing regimen, then followed by simulation with *E. coli* toxic LPS at the dose of 15 mg/kg (Fig. 1A). The survival time and rates in the ALOS-treated groups were significantly enhanced than those of the untreated group. Moreover, mice pre-treated with ALOS in a two-dose regimen showed superior protective activity to those receiving in the single dose of ALOS (Fig. 1B). ALOS pretreatment significantly reduced inflammatory factors, with the two-dose regimen being superior to the single dose (Figs. 1C-E). Flow cytometry analysis indicated that pretreatment with ALOS increases the proportion of macrophages and DCs in intestinal lamina propria (LP), mesenteric lymph node (MLN), peritoneal irrigation fluid (PLF), and spleen (Figs. S2A-B), inferring the systemically immune activation. ALOS also attenuated the immune stimulation induced by toxic LPS (Figs. S2C-D). Based on above results, we selected two-dose regiment for further investigation on sepsis model and compared with *E. coli* LPS at the dose of 0.2 mg/mL (Fig. 1F). Survival analysis demonstrated that both ALOS and *E. coli* LPS pre-treatments significantly prolonged mouse survival after challenging with the high dose of toxic LPS, while ALOS exhibited superior efficacy to *E. coli* LPS (Fig. 1G). In addition, ALOS reduced levels of plasma aspartate transaminase (AST), alanine transaminase (ALT), lactate dehydrogenase (LDH), urea, creatinine (CREA), and creatine kinase (CK) compared to mice in the *E. coli* LPS-pretreated group and the model (MOD) group (15 mg/kg *E. coli* LPS) (Figs. 1H-K, S3A-B). H&E staining revealed that ALOS conferred broad protection against multi-organ injuries (lung, liver, heart, kidney) (Figs. 1L, S3C). Specifically, ALOS alleviated alveolar damage, preserved hepatic lobular architecture with reduced lipid vacuolation, attenuated renal tubular edema, interstitial inflammation, and myocardial injury.

Moreover, we employed the cecal ligation and puncture (CLP) model to assess its efficacy in polymicrobial peritonitis (Fig. 1M). Consistently, ALOS significantly increased the survival time and decreased pathological injury across multiple organs in CLP mice (Figs. 1N-S, S3D-F). Collectively, these findings indicate that ALOS significantly alleviates multiorgan damage caused by LPS-induced lethal endotoxemia or CLP-induced peritonitis.

It has been previously shown that ALOS repairs the damaged intestinal epithelia by enhancing IL-22 production in DIO mice.[22] Building upon this, we first confirmed in naive C57BL/6J mice that ALOS elevated intestinal IL-22 and activated IL-22-dependent stem cell renewal, as indicated by upregulated Notch1, β-catenin, and LGR5(Figs. 2A-B). We further identified Group 3 innate lymphoid cells (ILC3s) as the primary cellular source of this secreted IL-22, a result replicated in both naïve C57BL/6J mice and sepsis models (Figs. 2C-E, S3G-H). Besides, ALOS treatment was found to upregulated genes related to the stem cell renewal pathway, increased tight junction proteins (*Tjp1*, *Ocln* and *Muc2*) and promoted the expression of antimicrobial peptides (AMPs) via the IL-22 (Figs. 2F-I, S3I-T). Given the pivotal roles of IL-22 and AMPs in maintaining mucosal homeostasis,[27-30] we next characterized the intestinal microbiome profile of ALOS-treated mice. Analysis of β-diversity and α-diversity indicated that ALOS significantly reshapes gut microbial composition (Figs. 2J-M). Furthermore, Manhattan plots and LEfSe analysis identified a specific enrichment of *Dubosiella sp00403415*, *Lactobacillus johnsonii*, and *Lachnospiraceae bacterium* (Figs. 2N-Q, S3U). Of note, some of these bacteria have been reported to possess anti-inflammatory properties.[31-35] Thus, ALOS is conductive to establish a gut microbiota benefiting for resisting inflammatory diseases.

To further determine the contribution of ALOS-induced gut microbiota to its protection against sepsis, we evaluated the efficacy of ALOS in pseudo-germ-free mice in which the gut microbiota was depleted by broad-spectrum antibiotics prior to LPS challenge (Figs. S4A). In the absence of an intact microbiota, ALOS pretreatment increased survival time, while significantly attenuating systemic inflammatory cytokine production, and reducing multi-organ injury (Figs. S4B-J). These findings demonstrate that ALOS can confer protection against sepsis independently of the gut microbiota. ALOS produces relatively weaker protection in pseudo-germ-free mice than in wild type mice, which combined with the immunomodulatory properties of ALOS, implicates that ALOS-induced gut microbiota may play auxiliary roles in the anti-sepsis effects of ALOS. The exact roles of gut bacteria enriched by ALOS needs to be validated by culturing strains and *in vivo* studies in the future.

ALOS reduces inflammatory cytokine storm and reverses immune imbalance.

The pathogenesis of sepsis is driven by a dysregulated immune response, leading to severe systemic inflammatory injuries. To evaluate whether ALOS effectively regulates the pathological hyperinflammation, we quantified serum cytokines in the LPS-induced and CLP sepsis models. ELISA analysis demonstrated that ALOS pretreatment

significantly reduced circulating levels of vital inflammatory factors: IL-6 decreased by 64.8%, IL-1β by 70.1%, and TNF-α by 65.3% relative to that in MOD group (Figs. 3A-C). Moreover, ALOS markedly attenuated the inflammatory response in pulmonary, hepatic, renal, and cardiac tissues (Figs. 3D, S5A-C). The anti-inflammatory effect of ALOS was also observed in the CLP model (Figs. 3E-H, S5D-F). Furthermore, we analyzed the phenotypic changes of macrophages in the intestinal LP and spleen by flow cytometry. An anti-inflammatory phenotype was observed in ALOS-pretreated sepsis mice, characterized by a decrease in pro-inflammatory ($CD86^+F4/80^+CD11b^+$) macrophages and an increase in anti-inflammatory ($CD206^+F4/80^+CD11b^+$) macrophages (Figs. 3I-J, S5G-H). This phenotypic shift was functionally corroborated by decreased TNF-α among pro-inflammatory macrophages and IL-10 in anti-inflammatory macrophages isolated from intestinal lamina propria cells (ILPs) (Figs. 3I-J).

Given the observed reprogramming of innate immunity by ALOS, we investigate its influence on the adaptive immunity, particularly the critical Th17/Treg balance. In both sepsis models, we observed a reduction in IL-17-producing T helper 17 (Th17) cells and a significant increase in $FoxP3^+$ regulatory T cells (Tregs) in the spleens and ILPs of ALOS-pretreated sepsis mice compared to those in the sepsis mice, thus rebalancing the dysregulated Th17/Treg ratio (Figs. 3K-P). These results suggest that ALOS reshapes the immune response, inducing anti-inflammatory and reparative phenotype.

ALOS induces semi-mature and hyporesponsive dendritic cells (DCs).

Having established that ALOS reprograms the immune response *in vivo*, we attempt to identify the upstream driver of this response. We focused on the isolated BMDCs, given their role as master regulators of adaptive immunity and their dysregulation is implicated in inflammatory diseases.[36] We analyzed the expression of surface markers on BMDCs following stimulation with either ALOS or *E. coli* LPS. (Figs. 4A and S6A). *E. coli* LPS has been reported to induce the maturation of DCs. As expected, *E. coli* LPS robustly upregulated the expression of surface markers MHC II, CD40, CD80, and CD86 on BMDCs. In comparison with the immunoregulatory effect of *E. coli* LPS, ALOS induced the generation of semi-mature dendritic cells (semi-DCs),[37, 38] as evidenced by the moderate increase of MHC II, CD40, CD80, and CD86 (Figs. 4B-F), which was also verified *in vivo* (Figs. S6B-E) and consistent with the relatively low levels of IL-6 and IL-1β (Figs. 4G-H). However, ALOS showed similar potency as *E. coli* LPS in stimulating the production of IL-10 in BMDCs (Fig. 4I).

Induction of semi-maturation in DCs can confer tolerance to subsequent toxic LPS stimulation.[12] Herein, the ALOS-primed BMDCs showed lower expression levels of MHC II, CD80, CD86, and CD40 and relatively low levels of TNF-α after toxic LPS challenge, as compared to non-primed BMDCs (Figs. 4J-O, S1D-E), supporting a tolerance towards *E. coli* LPS . These data together indicate that ALOS reprograms dendritic cells and induce a tolerant phenotype.

ALOS activates the IDO1-Kyn-AhR signaling pathway

To further investigate the mechanisms underlying ALOS-induced immune regulatory effects, we performed RNA-seq analysis on untreated BMDCs versus ALOS-treated BMDCs. Transcriptomic analysis revealed that ALOS-treated BMDCs significantly upregulated genes associated with immune tolerance, including *Ido1*, *Ido2*, *Bach2*, and *Pdcd1lg2,* etc. (Fig. 5A). Among these, *Ido2* encodes an indoleamine 2,3-dioxygenase 1(IDO1) homolog with lower catalytic activity, *Bach2* promotes Treg lineage stability, and *Pdcd1lg2* encodes the co-inhibitory ligand PD-L2. Their coordinate upregulation with Ido1 indicates a broad tolerogenic transcriptional reprogramming. IDO1, a rate-limiting enzyme that catabolizes tryptophan to generate kynurenine (Kyn), is the core regulator of DCs tolerance.[39] Indeed, gene expression involved in the tryptophan catabolic process was also elevated in ALOS-treated BMDCs (Fig. 5B). The following qPCR assay further confirmed the ALOS-upregulated mRNA expression of *Ido1* (Fig. 5C). Kyn works as an agonist for aryl hydrocarbon receptor (AhR) that regulates the tolerogenic dendritic cells and differentiation of Tregs.[31, 40] Consistent with the enhanced *Ido1* expression, ALOS significantly increased the production of Kyn, the mRNA levels of the Kyn transporter and AhR *in vitro* and *in vivo* (Figs. 5D-E, S7A-D). When knocking down the expression of *Ido1* in BMDCs, ALOS loses the ability to enhance the Kyn production (Figs. S7E-F). Furthermore, an exogenous addition of Kyn to BMDCs upregulated the mRNA levels of AhR (Fig. 5E). Immunofluorescence and western blot (WB) analysis confirmed that both ALOS and Kyn promoted the nuclear translocation of AhR, with AhR agonist FICZ serving as a positive control in the WB analysis. (Figs. 5F and S7G).

It has been reported that AhR deficiency results in decreased survival in *Serratia marcescens* sepsis model.[41] Next, we explore whether ALOS promotes the Tregs differentiation through the activation of AhR by employing a conditioned medium transfer assay (Fig. 5G). The conditioned medium from ALOS-treated BMDCs was used to incubate the induced Treg (iTreg) cells. Compared to the control medium, the ALOS-conditioned medium significantly increased the proportion of $Foxp3^{+}CD25^{+}$ Treg cells. Such enhancement was also reproduced by addition of Kyn in the control medium (Figs. 5H-I). Immunofluorescence revealed that ALOS-conditioned medium also enhanced the expression of AhR on Treg cells (Fig. 5J). Moreover, the AhR antagonist CH223191 (Fig. 5K) inhibited conditioned medium-induced $Foxp3^{+}$ Treg induction and AhR upregulation, and also significantly suppressed activation of its downstream effector CYP1A1(Fig. S7H). These data demonstrate the central role of Kyn-AhR axis in ALOS-induced Treg differentiation (Fig. S7I). Further, we co-cultured ALOS-primed BMDCs with naïve $CD4^{+}$ T cells under Treg-polarizing conditions. The co-culturing significantly increased the proportion of $CD25^{+}Foxp3^{+}$ Tregs in cells (Fig. S7J). This finding provides functional evidence that ALOS induces semi-mature tolerogenic DC.

The anti-sepsis effect of ALOS requires activation of IDO1

To further confirm the causal role of IDO1 in the protective effects of ALOS, we employed the IDO1 inhibitor NLG919 (Fig. 6A). NLG919 treatment abolished the protective effects of ALOS on the improvement in survival rate, pathophysiological indicators, inflammatory factors, as well as organ damage parameters (Figs. 6B-H and S8A). The ALOS-induced generation of Kyn, differentiation of Tregs, and rebalancing of the Th17/Treg ratio was also completely suppressed (Figs. 6I-K and S8B). These results indicate that IDO1 is necessary for the protective effect of ALOS against sepsis. On the other hand, administration of Kyn to septic mice elevated plasma Kyn levels and produced similar protective phenotype as that of ALOS (Figs. 6L-V and S8C). Pretreatment with Kyn significantly prolonged survival time and alleviates disease severity in septic mice, which was indicated by reduced inflammatory cytokines (IL-6, TNF-α), and organ dysfunction parameters (AST, ALT, CREA, CK, BUN). Similar to ALOS, Kyn significantly promoted the differentiation of Tregs, reestablished the balance between Th17/Treg (Figs. 6U-V and S8D). Additionally, Kyn significantly enhanced IL-22^{+} ILC3 population (Figs. S8E-F). AhR is a key transcriptional regulator of IL-22 in immune cells. Considering the role of Kyn as the ligand of AhR, the ALOS-induced production of IL-22 is deduced to a functionally downstream response of the ALOS-IDO1-Kyn-AhR axis. Altogether, these findings demonstrate that activation of IDO1 in immune cells is the key underlying mechanism for the protection of ALOS against sepsis.

Activation of TLR4-NF-κB signaling enhances the expression of IDO1 protein in DCs. Given that ALOS is a moderate TLR4 agonist, we used TLR4$^{-/-}$ mice to determine whether TLR4 is required for ALOS-mediated protection. ALOS pretreatment failed to suppress pro-inflammatory cytokine levels across multiple organs and conferred no survival benefit (Figs. S9A-F), demonstrating that TLR4 is indispensable for the anti-sepsis activity of ALOS.

Collectively, ALOS reprograms host immunity during sepsis by shifting a pro-inflammatory immune state toward an anti-inflammatory, disease-tolerant state. Mechanistically, ALOS targets TLR4 to induce semi-mature DCs, thereby triggering transcriptional activation of IDO1, IDO1-mediated Kyn production subsequently promotes Treg differentiation, thereby reducing inflammation and protecting tissue through the IDO1-Kyn-AhR axis.

ALOS exerts therapeutic effects in CLP sepsis model and safety in wild mice

To evaluate whether ALOS produces therapeutic efficacy, CLP mice was given ALOS intraperitoneally half an hour after surgery, alongside with model and ALOS-pretreated mice as control (Figs. S10A). Compared with CLP mice, mice receiving ALOS after onset of sepsis exhibited prolonged survival, reduced plasma TNF-α and IL-6 levels, and attenuated multi-organ injury, as evidenced by decreased organ damage biomarkers and diminished pulmonary and hepatic histopathology (Figs. S10B-J). Notably, the protective effects of ALOS in the therapeutic administration are weaker that those achieved in the prophylactic treatment.

To further assess the safety of ALOS administration, mice receiving ALOS via intraperitoneal injection for one week were observed, with an equivalent dose of *E. coli* LPS as control (Figs. S11A). The *E. coli* LPS-treated mice showed marked weight loss, significantly elevated plasma inflammatory cytokines and organ injury biomarkers, dramatically increased pulmonary and hepatic damage, colon shortening, and inflammatory infiltration (Figs. S11B-L). In contrast, ALOS-treated mice showed little impact on body weight, slight increase in inflammation and little organ damage. These data demonstrate that ALOS has a favorable safety profile under repeated dosing.

ALOS mitigates hyperinflammation, organ injury, and improves survival in a porcine sepsis model.

Pigs share much similarity in the physiological and immunological properties with human. To further reveal the clinical potential of ALOS in treating sepsis, we used the porcine sepsis model to assess the protective effects of ALOS.[42] The experimental framework is shown in Fig. 7A. The ALOS-pretreated group exhibited significantly longer survival compared to the MOD mice (Fig. 7B). Biochemical profiling revealed that ALOS reduced serum AST, ALT, BUN, and CK (Figs. 7C-F). In addition, ALOS profoundly suppressed the levels of serum IL-6, TNF-α, and C-reactive protein (Figs. 7G-I). These systemic anti-inflammatory effects ultimately achieved the protective effect, as evidenced by significantly attenuated histopathological lesion scores across the liver, kidneys, lungs, and heart in the ALOS-treated group (Figs. 7J-M). The key inflammatory factors, such as proinflammatory cytokines (IL-6, TNF-α) and C motif chemokine ligands (Ccl2, Ccl3), were also reduced in these tissues by ALOS pretreatment (Figs. 7J-M). As observed in the murine model, the level of Kyn in plasma was significantly increased by ALOS (Fig. S12A), which implicated the same underlying mechanism in piglets as that corroborated in mice.

Discussion

A. muciniphila has been documented as a dominant commensal bacterium colonizing the mucous layer of intestinal tract.[43-45] It has attracted considerable attention due to its diverse beneficial roles in metabolic and inflammatory diseases.[46-48] However, the mechanisms underlying these effects remain inadequately elucidated. In our previous study, we demonstrated that intraperitoneal administration of the ALOS effectively ameliorated obesity and its related disorders in IL-22 dependent manner.[22] In this study, we demonstrated that pretreatment with ALOS protects host against LPS- or CLP-induced lethal sepsis. ALOS pretreatment reprograms host immunity to suppress pathological inflammation and enhance immunological tolerance. This immune reprogramming involves the induction of semi-DC and activation of the IDO1-Kyn-AhR axis, which subsequently promotes Treg differentiation. The fact that ALOS produced comparable efficacy in both models further supports the concept that ALOS acts primarily by boosting host disease tolerance rather than by simply suppressing inflammatory pathway or pathogens. ALOS administrated after onset of sepsis also

provided considerable protection.

A number of gut commensal-derived LOS have been identified with immunomodulatory properties,[49-51] such as *Segatella copri* LOS acting via TLR2/1,[52] *Bacteroides thetaiotaomicron* LOS signaling through TLR2 with minimal engagement of the MD-2/TLR4 pathway,[53] and *B. eggerthii* LOS weakly activating TLR4 to induce semi-mature dendritic cells, but their protective roles in sepsis and the underlying mechanisms remain incompletely clarified.[51] Our study demonstrates that ALOS is mechanistically distinct by uniquely coupling moderate TLR4 agonism to transcriptional activation of IDO1, thereby initiating the Kyn-AhR axis as the major immune mechanism. In early studies, *B. vulgatus* LPS and *B. fragilis* lipid A moiety of LPS were reported to promote Treg cells through cathepsin S or sustained IFN-β production, respectively. [12, 13] Herein, ALOS relies on IDO1-generated Kyn to simultaneously drive Treg differentiation and suppress Th17 responses. Unlike TLR4 antagonists such as Eritoran that merely block signaling,[16] ALOS actively reprograms dendritic cells toward a tolerogenic state. Furthermore, although the IDO1-Kyn-AhR pathway was implicated in intestinal homeostasis modulated by *Dubosiella newyorkensis*,[31] our findings establish the link between a defined microbial LOS and systemic activation of this axis in sepsis, where Kyn acts on both dendritic cells and T cells while coordinating IL-22-mediated barrier protection. This integrated immunometabolic regulation distinguishes ALOS from previously described LOS/LPS immunomodulators. The beneficial immunological activity of ALOS could be ascribed to their unique chemical structures. Eight *Akkermansia* species in gut has been recently identified by genome sequencing analysis.[54] A comprehensive investigation of the chemical and immune traits of LOS from different *Akkermansia* species would help elucidate structure-activity relationship.

The key immunomodulatory feature of ALOS lies in its ability to induce a semi-mature, tolerogenic state in DCs by providing a moderate activation signal that avoids the excessive production of pro-inflammatory cytokines.[55, 56] Dysregulated activation or maturation of DCs lead to excessive immune responses, aggravating inflammatory diseases. Compared with mature DCs induced by *E. coli* LPS, ALOS induced a semi-mature state in DCs. The semi-mature activation is the key feature of regulatory dendritic cells, with appropriately increased expression of MHC class II and co-stimulatory molecules like CD80/86, which further induce differentiation of Tregs.[57] Gut commensal bacteria and their bioactive substance have been reported to modulate the immune functions of DCs.[58] Probiotics *L. rhamnosus* and *L. delbrueckii* promote tolerogenic phenotypes in DCs by decreasing the expression of co-stimulatory molecules such as CD40, CD86, CD80, and HLA-DR during the maturation process and enhance the differentiation of Tregs.[59-61] S-layer proteins from *L. acidophilus* bind to DC-SIGN on DCs, triggering the secretion of IL-10 and promoting a regulatory DC phenotype.[62] *B. vulgatus* LPS induces semi-mature $CD11c^{+}$ cells in the intestinal LP, contributing to prevention of colitis.[12] ALOS induces semi-mature DCs, producing a tolerant phenotype to the toxic LPS challenge in sepsis. Given the expression of TLR4 on distinct immune cell types, we cannot rule out that ALOS may

also act on other immune cells, such as macrophages or neutrophils, whose contributions to ALOS-mediated protection remain to be elucidated.

Ido1 encoding the rate-limiting enzyme in the kynurenine pathway ranked among the immune tolerance-associated genes upregulated by ALOS. As a downstream product of IDO1 pathway, Kyn orchestrates multiple immunomodulatory functions through activating AhR. It not only activates AhR in DCs, increasing the expression of IDO1,[63] but also interacts with AhR in T cells to promote T-cell differentiation toward $FoxP3^+$ Tregs over Th17 cells.[40] In addition, we detected that the ALOS enhanced the proportion of $IL\text{-}22^+$ ILC3s in LP, which is possibly linked with activation of Kyn-AhR axis. The intestinal IL-22 helps maintaining the gut barrier functions by promoting stem cell markers and controlling gut pathogens by secreting antimicrobial peptides, contributing to protection against sepsis.[64] The dysregulated Th17/Treg ratio is one of important immune dysfunction characteristics in sepsis.[65, 66] ALOS restored the Th17/Treg balance in both LPS-induced and CLP sepsis models via the IDO1-Kyn-AhR axis. Functional experiments establish the IDO1-Kyn-AhR axis as the main mechanism for ALOS-mediated immune reprogramming. Tryptophan catabolism generates indole derivatives other than Kyn, and the contributions of these additional metabolites cannot be ruled out based on the current data.

To evaluate the clinical value of ALOS, an LPS-induced porcine sepsis model was established. Pretreatment with ALOS significantly prolonged survival time and alleviated inflammatory damage, indicating the potential clinical value of ALOS. However, the porcine endotoxemia model does not fully recapitulate infection-driven clinical sepsis, which warrants further studies in infection-associated models and human cohorts. The mixture characteristics of ALOS hinders investigation on the dynamic interaction between ALOS and its receptor TLR4-MD-2, as well as its effect on the LPS affinity. Furthermore, comparative analysis of ALOS and other commensal bacterial LOS variants remained to be delineated. The intraperitoneal regimen used in this work has some clinical limitations. The intravenous administrating route or encapsulation-based oral delivery should be considered in the future assay. In addition, fecal microbiota transplantation experiment and assay with IDO1 knockout mice need to be conducted, corroborating the roles of gut microbiota and the IDO1-Kyn-AhR axis in reducing sepsis. Future work addressing these limitations will enhance the clinical translation of ALOS preparation.

With regard to its clinical relevance, more investigations are required to test the efficacy and safety of ALOS. Similar to glucocorticoids, ALOS may be used as an immunomodulator in high-risk situations. Patients undergoing major abdominal surgery and large area of burns are at substantially elevated risk. In such settings, prophylactic treatment with immune-modulators is clinically feasible and valuable. In addition, this approach also holds promise in veterinary and livestock settings, such as preventing sepsis in weaning piglets.

Conclusion

In conclusion, our findings establish ALOS as an immunomodulatory postbiotic that reprograms dendritic cell maturation and T cell balance, thereby mitigating hyperinflammation and enhancing disease tolerance in sepsis. The translational relevance is validated in a porcine model, underscoring the therapeutic potential of microbial glycolipids for acute inflammatory disorders.

Conflict of Interest

The authors declare no conflict of interest.

References

1. M. Cecconi, L. Evans, M. Levy, A. Rhodes. Sepsis and septic shock. The Lancet. 2018;392(10141):75-87.

2. R. Salomão, B.L. Ferreira, M.C. Salomão, S.S. Santos, L.C.P. Azevedo, M.K.C. Brunialti. Sepsis: evolving concepts and challenges. BRAZ J MED BIOL RES. 2019;52(4):e8595.

3. J.-L. Vincent, J. Rello, J. Marshall, E. Silva, A. Anzueto, C.D. Martin, et al. International study of the prevalence and outcomes of infection in intensive care units. JAMA. 2009;302(21):2323-9.

4. S. Karlsson, M. Varpula, E. Ruokonen, V. Pettilä, I. Parviainen, T.I. Ala-Kokko, et al. Incidence, treatment, and outcome of severe sepsis in ICU-treated adults in Finland: the Finnsepsis study. INTENS CARE MED. 2007;33(3):435-43.

5. M. Cao, G. Wang, J. Xie. Immune dysregulation in sepsis: experiences, lessons and perspectives. Cell Death Discov. 2023;9(1):465.

6. J.J. De Waele. Importance of timely and adequate source control in sepsis and septic shock. J Intensive Med. 2024;4(3):281-6.

7. D. Liu, S.Y. Huang, J.H. Sun, H.C. Zhang, Q.L. Cai, C. Gao, et al. Sepsis-induced immunosuppression: mechanisms, diagnosis and current treatment options. Mil Med Res. 2022;9(1):56.

8. E.J. Giamarellos-Bourboulis, A.C. Aschenbrenner, M. Bauer, C. Bock, T. Calandra, I. Gat-Viks, et al. The pathophysiology of sepsis and precision-medicine-based immunotherapy. Nat Immunol. 2024;25(1):19-28.

9. F. Di Lorenzo, C. De Castro, A. Silipo, A. Molinaro. Lipopolysaccharide structures of Gram-negative populations in the gut microbiota and effects on host interactions. FEMS Microbiol Rev. 2019;43(3):257-72.

10. S. Salminen, M.C. Collado, A. Endo, C. Hill, S. Lebeer, E.M.M. Quigley, et al. The International Scientific Association of Probiotics and Prebiotics (ISAPP) consensus statement on the definition and scope of postbiotics. Nat Rev Gastroenterol Hepatol. 2021;18(9):649-67.

11. H. Fang, E.L.R. Rodrigues, N.G. Barra, D. Kukje Zada, N. Robin, A. Mehra, et al. Postbiotic impact on host metabolism and immunity provides therapeutic potential in metabolic disease. Endocr Rev. 2025;46(1):60-79.

12. A. Steimle, L. Michaelis, F. Di Lorenzo, T. Kliem, T. Münzner, J.K. Maerz, et al. Weak agonistic LPS restores intestinal immune homeostasis. Mol Ther. 2019;27(11):1974-91.

13. H.S. Cho, J.S. Yoo, X. Song, B. Goh, A. Diallo, J. Lee, et al. Structure of gut microbial glycolipid modulates host inflammatory response. Cell. 2025;188(19):5295-312.

14. H.C. Lai, T.L. Lin, T.W. Chen, Y.L. Kuo, C.J. Chang, T.R. Wu, et al. Gut microbiota modulates COPD pathogenesis: role of anti-inflammatory *Parabacteroides goldsteinii* lipopolysaccharide. Gut. 2022;71(2):309-21.

15. G. Malgorzata-Miller, L. Heinbockel, K. Brandenburg, J.W.M. van der Meer, M.G. Netea, L.A.B. Joosten. *Bartonella quintana* lipopolysaccharide (LPS): structure and characteristics of a potent TLR4 antagonist for in-vitro and in-vivo applications. Sci Rep. 2016;6(1):34221.

16. A. Barochia, S. Solomon, X. Cui, C. Natanson, P.Q. Eichacker. Eritoran tetrasodium (E5564) treatment for sepsis: review of preclinical and clinical studies. EXPERT OPIN DRUG MET. 2011;7(4):479-94.

17. I.D. Iliev, J.M. Blander, N. Collins, C.-J. Guo, R.S. Longman, G.F. Sonnenberg, et al. Microbiota-mediated mechanisms of mucosal immunity across the lifespan. Nat Immunol. 2025;26(10):1645-59.

18. S. Xie, J. Li, F. Lyu, Q. Xiong, P. Gu, Y. Chen, et al. Novel tripeptide RKH derived from *Akkermansia muciniphila* protects against lethal sepsis. Gut. 2024;73(1):78-91.

19. J. Sun, X. Ding, S. Liu, X. Duan, H. Liang, T. Sun. Adipose-derived mesenchymal stem cells attenuate acute lung injury and improve the gut microbiota in septic rats. Stem Cell Res Ther. 2020;11(1):384.

20. B. Han, K. Chao, D. Wang, Y. Sun, X. Ding, X. Zhang, et al. A purified membrane protein from *Akkermansia muciniphila* blunted the sepsis-induced acute lung injury by modulation of gut microbiota in rats. Int Immunopharmacol. 2023;121.

21. J. Xie, H. Li, X. Zhang, T. Yang, M. Yue, Y. Zhang, et al. *Akkermansia muciniphila* protects mice against an emerging tick-borne viral pathogen. Nat Microbiol. 2023;8(1):91-106.

22. L. Sun, Y. Zhang, W. Dong, J. Sun, T. Wang, F. Shao, et al. *Akkermansia muciniphila*-derived hypoacylated rough-type lipopolysaccharides alleviate diet-induced obesity via activation of TLR4−IL-23−IL-22 immune axis. iMeta. 2025;4(5):70066.

23. Y. Zhang, W. Dong, J. Lin, J. Sun, R. Yin, X. Lv, et al. Diversity of oligosaccharides in lipooligosaccharides of *Akkermansia muciniphila* and its anti-atherosclerotic activity. Nat Prod Bioprospect. 2026;16(1):58.

24. H. Schneider, T.L. Hale, W.D. Zollinger, R.C. Seid, Jr., C.A. Hammack, J.M. Griffiss. Heterogeneity of molecular size and antigenic expression within

lipooligosaccharides of individual strains of *Neisseria gonorrhoeae* and *Neisseria meningitidis*. Infect Immun. 1984;45(3):544-9.

25. F.F. Anhê, N.G. Barra, J.F. Cavallari, B.D. Henriksbo, J.D. Schertzer. Metabolic endotoxemia is dictated by the type of lipopolysaccharide. Cell Rep. 2021;36(11):109691.

26. G.M. de Tejada, L. Heinbockel, R. Ferrer-Espada, H. Heine, C. Alexander, S. Bárcena-Varela, et al. Lipoproteins/peptides are sepsis-inducing toxins from bacteria that can be neutralized by synthetic anti-endotoxin peptides. Sci Rep. 2015;5(1):14292.

27. A. Abdelgawad, T. Nicola, I. Martin, B.A. Halloran, K. Tanaka, C.Y. Adegboye, et al. Antimicrobial peptides modulate lung injury by altering the intestinal microbiota. Microbiome. 2023;11(1):226.

28. S.J. Aujla, Y.R. Chan, M. Zheng, M. Fei, D.J. Askew, D.A. Pociask, et al. IL-22 mediates mucosal host defense against Gram-negative bacterial pneumonia. Nat Med. 2008;14(3):275-81.

29. Y. Zheng, P.A. Valdez, D.M. Danilenko, Y. Hu, S.M. Sa, Q. Gong, et al. Interleukin-22 mediates early host defense against attaching and effacing bacterial pathogens. Nat Med. 2008;14(3):282-9.

30. M.O. Jakob, D. Spari, D. Sànchez Taltavull, L. Salm, B. Yilmaz, R. Doucet Ladevèze, et al. ILC3s restrict the dissemination of intestinal bacteria to safeguard liver regeneration after surgery. Cell Rep. 2023;42(3):112269.

31. Y. Zhang, S. Tu, X. Ji, J. Wu, J. Meng, J. Gao, et al. *Dubosiella newyorkensis* modulates immune tolerance in colitis via the L-lysine-activated AhR-IDO1-Kyn pathway. Nat Commun. 2024;15(1):1333.

32. X. Fan, C. Mai, L. Zuo, J. Huang, C. Xie, Z. Jiang, et al. Herbal formula BaWeiBaiDuSan alleviates polymicrobial sepsis-induced liver injury via increasing the gut microbiota *Lactobacillus johnsonii* and regulating macrophage anti-inflammatory activity in mice. Acta Pharmaceutica Sinica B. 2023;13(3):1164-79.

33. S. Tao, M. Song, J. Fan, F. Zhu, T. Lv, H. Wei. *Lactobacillus johnsonii*-derived extracellular vesicles carrying GAPDH protect against ulcerative colitis through modulating macrophage polarization. J Adv Res. 2025;81:409-24.

34. D.J. Jia, Q.W. Wang, Y.Y. Hu, J.M. He, Q.W. Ge, Y.D. Qi, et al. Lactobacillus johnsonii alleviates colitis by TLR1/2-STAT3 mediated CD206(+) macrophages(IL-10) activation. Gut Microbes. 2022;14(1):2145843.

35. S. Deng, H. Cao, T. Li, X. Wang, J. Meng, T. Zeng, et al. Lachnospiraceae-bacterium alleviates ischemia-reperfusion injury in steatotic donor liver by inhibiting ferroptosis via the Foxo3-Alox15 signaling pathway. Gut Microbes.

2025;17(1):2460543.

36. A.T. Satpathy, X. Wu, J.C. Albring, K.M. Murphy. Re(de)fining the dendritic cell lineage. Nat Immunol. 2012;13(12):1145-54.

37. A. Steimle, K. Gronbach, B. Beifuss, A. Schäfer, R. Harmening, A. Bender, et al. Symbiotic gut commensal bacteria act as host cathepsin S activity regulators. J AUTOIMMUN. 2016;75:82-95.

38. O. Morante-Palacios, F. Fondelli, E. Ballestar, E.M. Martínez-Cáceres. Tolerogenic dendritic cells in autoimmunity and inflammatory diseases. Trends In Immunology. 2021;42(1):59-75.

39. C. Bello, P.P. Heinisch, M. Mihalj, T. Carrel, M.M. Luedi. Indoleamine-2,3-dioxygenase as a perioperative marker of the immune system. Front Physiol. 2021;12:766511.

40. J.D. Mezrich, J.H. Fechner, X. Zhang, B.P. Johnson, W.J. Burlingham, C.A. Bradfield. An interaction between kynurenine and the aryl hydrocarbon receptor can generate regulatory T cells. J Immunol. 2010;185(6):3190-8.

41. R.C. Keskey, J. Xiao, S. Hyoju, A. Lam, D. Kim, A.M. Sidebottom, et al. Enterobactin inhibits microbiota-dependent activation of AhR to promote bacterial sepsis in mice. Nat Microbiol. 2025;10(2):388-404.

42. J.K. Lunney, A. Van Goor, K.E. Walker, T. Hailstock, J. Franklin, C. Dai. Importance of the pig as a human biomedical model. Sci Transl Med. 2021;13(621):eabd5758.

43. P. Jiang, S. Ji, D. Su, Y. Zhao, V.B.E. Goncalves, G. Xu, et al. The biofunction of *Akkermansia muciniphila* in intestinal-related diseases. MRR. 2024;3(4):47.

44. P.D. Cani, C. Depommier, M. Derrien, A. Everard, W.M. de Vos. *Akkermansia muciniphila*: paradigm for next-generation beneficial microorganisms. Nat Rev Gastroenterol Hepatol. 2022;19(10):625−37.

45. A. Ioannou, M.D. Berkhout, S.Y. Geerlings, C. Belzer. *Akkermansia muciniphila*: biology, microbial ecology, host interactions and therapeutic potential. Nat Rev Microbiol. 2025;23(3):162-77.

46. H.S. Yoon, C.H. Cho, M.S. Yun, S.J. Jang, H.J. You, J.H. Kim, et al. *Akkermansia muciniphila* secretes a glucagon-like peptide-1-inducing protein that improves glucose homeostasis and ameliorates metabolic disease in mice. Nat Microbiol. 2021;6(5):563-73.

47. M. Zheng, R. Han, Y. Yuan, Y. Xing, W. Zhang, Z. Sun, et al. The role of *Akkermansia muciniphila* in inflammatory bowel disease: current knowledge and

perspectives. Front Immunol. 2022;13:1-19.

48. L. Wang, L. Tang, Y. Feng, S. Zhao, M. Han, C. Zhang, et al. A purified membrane protein from *Akkermansia muciniphila* or the pasteurised bacterium blunts colitis associated tumourigenesis by modulation of $CD8^+$ T cells in mice. Gut. 2020;69(11):1988-97.

49. K. Brunner, C.M. John, N.J. Phillips, D.G. Alber, M.R. Gemmell, R. Hansen, et al. Novel *Campylobacter concisus* lipooligosaccharide is a determinant of inflammatory potential and virulence. Lipid Res. 2018;59(10):1893-905.

50. P. Garcia-Vello, H.L.P. Tytgat, J. Elzinga, M. Van Hul, H. Plovier, M. Tiemblo-Martin, et al. The lipooligosaccharide of the gut symbiont *Akkermansia muciniphila* exhibits a remarkable structure and TLR signaling capacity. Nat Commun. 2024;15(1):8411.

51. M. Tiemblo Martín, M. Coccimiglio, E. Andretta, L. De Simone Carone, A. Bell, T. Gerpe-Amor, et al. The human gut *Bacteroides eggerthii* expresses a new galactofuranose-containing lipooligosaccharide with weak immunostimulatory properties. Carbohydr Polym. 2025;348:122833.

52. L. De Simone Carone, G. Barra, R. Cirella, M. Ziaco, M. Mercogliano, F. Olmeo, et al. Decoding a gut commensal signal: structural and immunological profiling of *Segatella Copri* lipopolysaccharide. Angew Chem Int Ed. 2025;64(48):202512947.

53. M.D. Pither, A. Illiano, C. Pagliuca, A. Jacobson, G. Mantova, A. Stornaiuolo, et al. *Bacteroides thetaiotaomicron* rough-type lipopolysaccharide: The chemical structure and the immunological activity. Carbohydr Polym. 2022;297:120040.

54. S. Ndongo, N. Armstrong, D. Raoult, P.-E. Fournier. Reclassification of eight *Akkermansia muciniphila* strains and description of *Akkermansia massiliensis* sp. nov. and Candidatus *Akkermansia timonensis*, isolated from human feces. Sci Rep. 2022;12(1):21747.

55. C. Qian, X. Cao. Dendritic cells in the regulation of immunity and inflammation. Semin Immunol. 2018;35:3-11.

56. J. Fucikova, L. Palova-Jelinkova, J. Bartunkova, R. Spisek. Induction of tolerance and immunity by dendritic cells: mechanisms and clinical applications. Front Immunol. 2019;10.

57. H.R. Christensen, H. Frøkiær, J.J. Pestka. *Lactobacilli* differentially modulate expression of cytokines and maturation surface markers in murine dendritic cells. J Immunol. 2002;168(1):171-8.

58. S. Baradaran Ghavami, H. Asadzadeh Aghdaei, D. Sorrentino, S. Shahrokh, M. Farmani, F. Ashrafian, et al. Probiotic-induced tolerogenic dendritic cells: A novel

therapy for inflammatory bowel disease? Int J Mol Sci. 2021;22(15).

59. H.-K. Kwon, C.-G. Lee, J.-S. So, C.-S. Chae, J.-S. Hwang, A. Sahoo, et al. Generation of regulatory dendritic cells and $CD4^{+}Foxp3^{+}$ T cells by probiotics administration suppresses immune disorders. PNAS. 2010;107(5):2159-64.

60. A.L. Hart, K. Lammers, P. Brigidi, B. Vitali, F. Rizzello, P. Gionchetti, et al. Modulation of human dendritic cell phenotype and function by probiotic bacteria. Gut. 2004;53(11):1602-9.

61. S.A. Esmaeili, M. Mahmoudi, Z. Rezaieyazdi, M. Sahebari, N. Tabasi, A. Sahebkar, et al. Generation of tolerogenic dendritic cells using *Lactobacillus rhamnosus* and *Lactobacillus delbrueckii* as tolerogenic probiotics. Cell Biochem. 2018;119(9):7865-72.

62. S.R. Konstantinov, H. Smidt, W.M. de Vos, S.C.M. Bruijns, S.K. Singh, F. Valence, et al. S layer protein A of *Lactobacillus acidophilus* NCFM regulates immature dendritic cell and T cell functions. PNAS. 2008;105(49):19474-9.

63. N.T. Nguyen, A. Kimura, T. Nakahama, I. Chinen, K. Masuda, K. Nohara, et al. Aryl hydrocarbon receptor negatively regulates dendritic cell immunogenicity via a kynurenine-dependent mechanism. PNAS. 2010;107(46):19961-6.

64. F. Deng, J.-J. Hu, Z.-B. Lin, Q.-S. Sun, Y. Min, B.-C. Zhao, et al. Gut microbe-derived milnacipran enhances tolerance to gut ischemia/reperfusion injury. Cell Rep Med. 2023;4(3):100979.

65. X. Liu, L. Chen, W. Peng, H. Deng, H. Ni, H. Tong, et al. Th17/Treg balance: the bloom and wane in the pathophysiology of sepsis. Front Immunol. 2024;15:1356869.

66. X. Chen, X. Chen, Y. Yang, N. Luo, J. Yang, L. Zhong, et al. Protective role of the novel cytokine Metrnl/ interleukin-41 in host immunity defense during sepsis by promoting macrophage recruitment and modulating Treg/Th17 immune cell balance. CLIN IMMUNOL. 2023;254:109690.

Figure 1

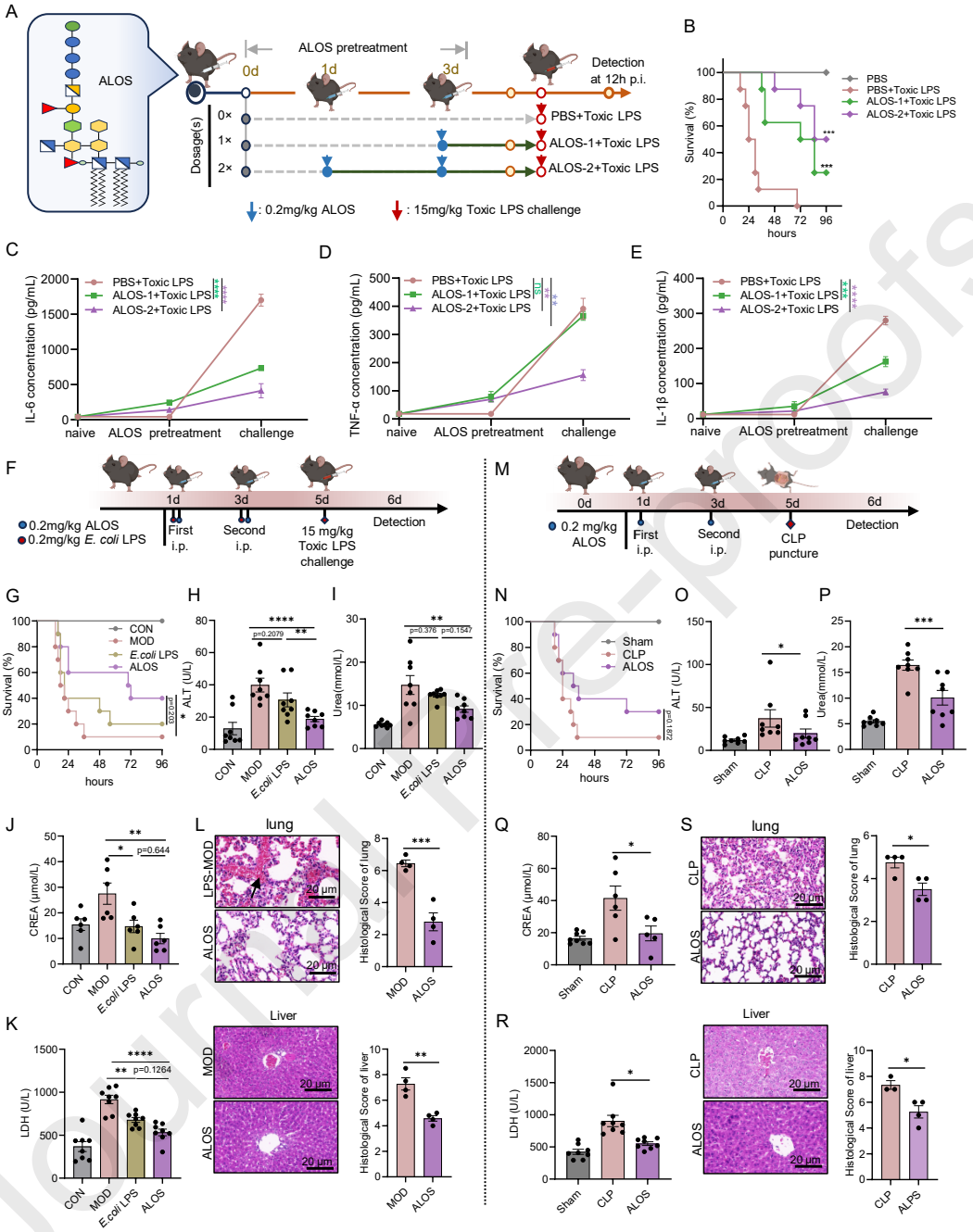

Fig. 1. ALOS confers protection in murine models. (A) Schematic diagrams of the ALOS structure and *in vivo* dosing regimens. Mice were administered with ALOS at day 1/3 days (two time, ALOS-2), and 3 days (two time, ALOS-1) for survival and cytokines assay. ALOS: *Akkermansia muciniphila*-derived lipooligosaccharides. Toxic LPS: 15mg/kg *Escherichia coli* LPS. (B) Survival rate of toxic LPS induced model, related to (A). (C-E) Dynamics of the inflammatory cytokines responses, related to (A): Interleukin-6 (IL-6) (C), Tumor necrosis factor alpha (TNF-α) (D), and interleukin-1β (IL-1β) (E) in the toxic LPS-induced model. (F) Experimental design showing groups

and durations in LPS-induced septic model. (G) Survival rate of toxic LPS-induced model. (H-K) The changes in biochemical indicators of plasma, including alanine aminotransferase (ALT) (H), Urea (I), and creatinine (CREA) (J), and lactate dehydrogenase (LDH) (K) in LPS-induced septic model. (L) H&E-stained images of pathological lung and liver in LPS-induced septic model (scale bar, 20μm). (M) Experimental design showing groups and durations in CLP-induced septic model. CLP: Cecum ligation and puncture. (N) Survival rate of CLP-induced septic model. (O-R) The changes in biochemical indicators of plasma, including ALT (O), Urea(P), and CREA (Q), and LDH(R) in LPS-induced septic model. (S) H&E-stained images of pathological lung and liver in CLP-induced septic model (scale bar, 20μm). *$p<0.05$, **$p<0.01$, ***$p<0.001$, ****$p<0.0001$,ns $p>0.05$ (Mantel- Cox log- rank test in B,G,N; One-way ANOVA in C-E, H-K, P, Q; the Kruskal–Wallis test in O, R; unpaired two-tailed Student's t- test in L, S. Results were expressed as the mean±SEM). n values: (L, R) n=4, (J, Q) n=6, (B, H, I, K, O, P, S) n=8, (G, N) n=10.

Figure 2

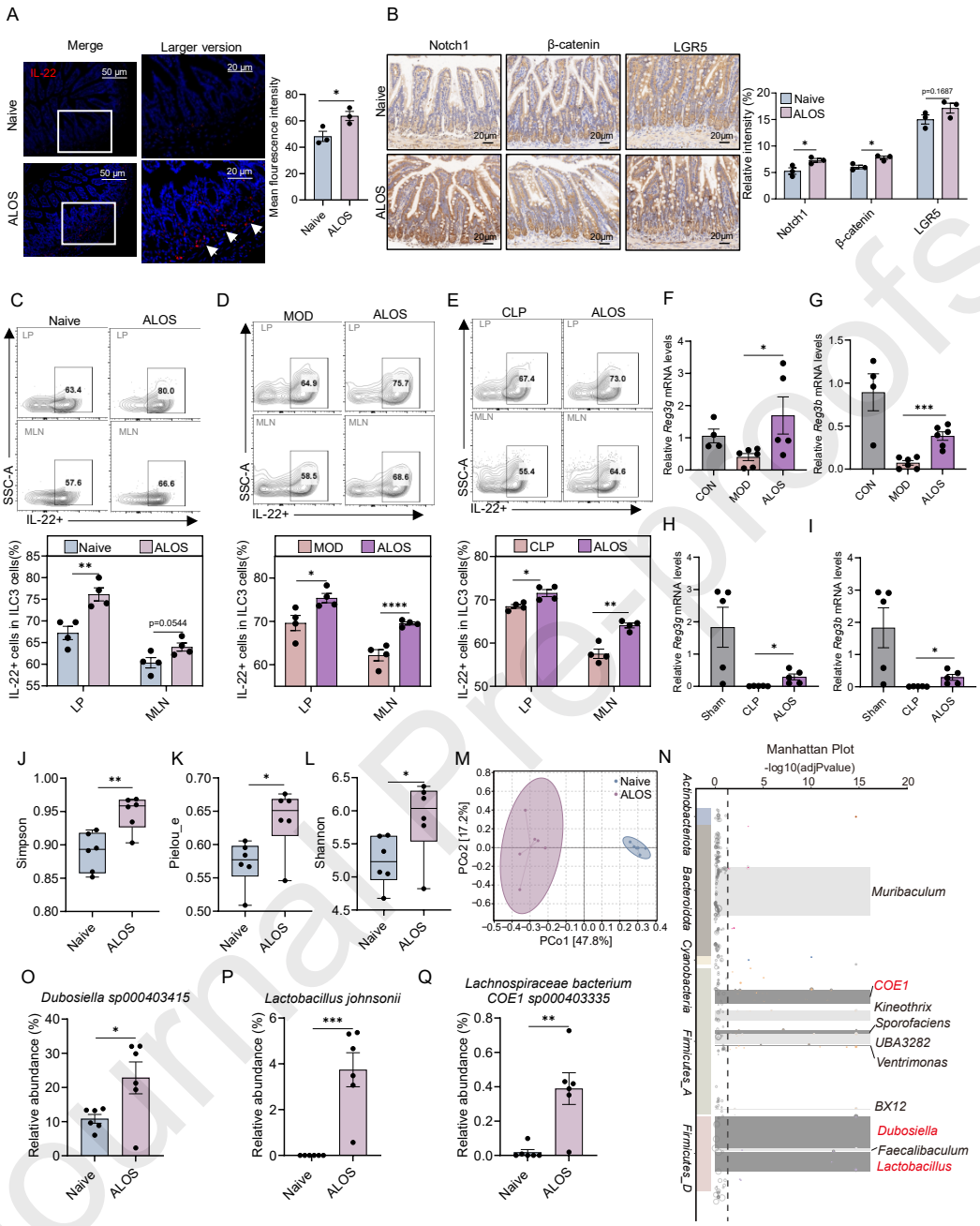

Fig. 2. ALOS regulates intestinal barrier homeostasis through IL-22. (A-C) Intestinal tissues were collected from the naïve C57BL/6J mice treated by ALOS and were used to perform cell flow cytometry detection, immunofluorescent staining and immunohistochemical staining. (A) The expression of IL-22 in the intestinal LP. (B) The expression of Notch1, β-catenin, LGR5 in the intestinal LP. (C) The proportion of IL-22^{+} ILC3 in naïve C57BL/6J. (D-I) Intestinal tissues were collected from septic models treated by ALOS. Proportions of IL-22+ ILC3s in LPS-(D) and CLP-induced sepsis models(E). Expression levels of antimicrobial peptides *Reg3g*(F), *Reg3b*(G) in LPS-induced sepsis model. Expression levels of antimicrobial peptides *Reg3g*(H),

Reg3b(I) in CLP-induced sepsis model. (J-L) Box plot of the Simpson index(J), Pielou_e index(K), Shannon index(L) represent α diversity for intestinal microbiota from the indicated treatment groups. (M) Unconstrained principal coordinate analysis (PCoA) with Bray-Curtis distance indicates microbial community differences (variation) across treatments. Ellipses represent a 95% CI around the cluster centroid. (N) Differential ASVs between Naive and ALOS group with the FDR < 0.05 were exhibited by Manhattan plot. (O) The relative abundance of *Dubosiella sp000403415*. (P) The relative abundance of *Lactobacillus johnsonii*. (Q) The relative abundance of *Lachnospiraceae bacterium COE1*. *p<0.05, **p<0.01, ***p<0.001, ****p<0.0001, ns p>0.05 (unpaired two-tailed Student's t-test in A-L, O-Q. Results were expressed as the mean ± SEM). n values: (A, B, D) n=3, (C, E) n=4, (F-Q) n=5.

Figure 3

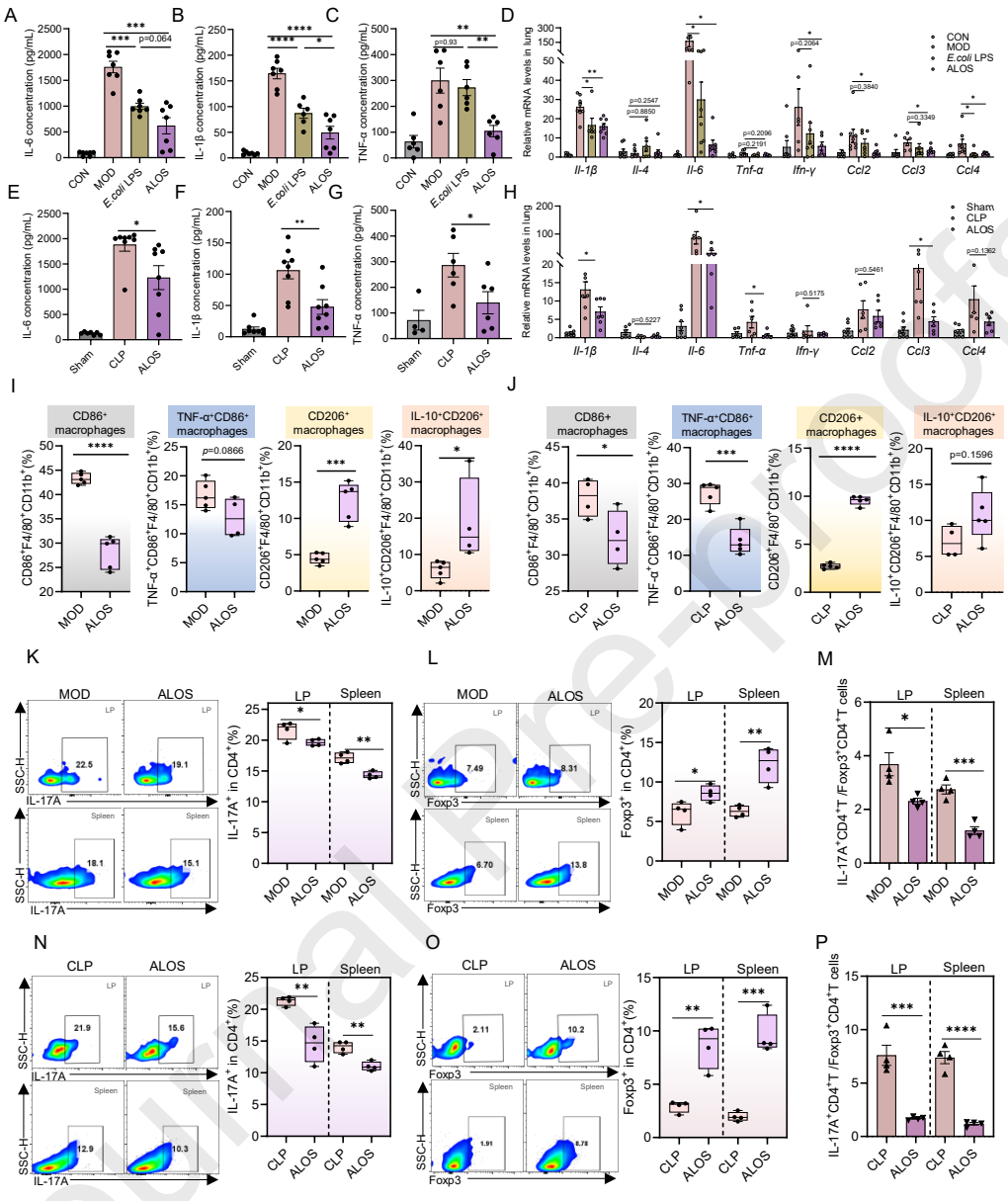

Fig. 3. ALOS inhibits inflammatory cytokines and reverses the immune imbalance in septic models. (A-C) The plasma concentration of inflammatory cytokines IL-6(A), IL-1β(B), TNF-α(C) in LPS-induced model. (D) mRNA expression level of inflammatory cytokines in lung of LPS-induced model. (E-G) The plasma concentration of inflammatory cytokines IL-6(E), IL-1β(F), TNF-α(G) in CLP-induced model. (H) mRNA expression levels of inflammatory cytokines in lung of CLP-induced model. (I) Changes in macrophage subsets in the LP tissue of LPS-induced model. (J) Changes in macrophage subsets in the LP tissue of CLP-induced model. (K-M) Changes in balance of Th17 and Treg in LPS-induced model. (K) The proportion of Th17 cells ($IL\text{-}17A^+$) in the LP and spleen tissues. (L)The proportion of Treg cells ($Foxp3^+$) in the LP and spleen tissues. (M) ratio of Th17/Treg in LPS-induced model. (N-P) Changes in balance

of Th17 and Treg in CLP-induced model. (N) The proportion of Th17 cells (IL-17A^{+}) in the LP and spleen tissues. (O)The proportion of Treg cells (Foxp3^{+}) in the LP and spleen tissues. (P) ratio of Th17/Treg in CLP-induced model. *p<0.05, **p<0.01, ***p<0.001, ****p<0.0001, ns p>0.05 (One-way ANOVA in A-C; Kruskal–Wallis test in D; Mann–Whitney U test in H; unpaired two- tailed Student's t- test in E-G, I-P. Results were expressed as the mean ± SEM). n values: (I-P) n=4, (D, H) n=6~8, (C, G) n=6, (A, B) n=7, (E, F) n=8.

Figure 4

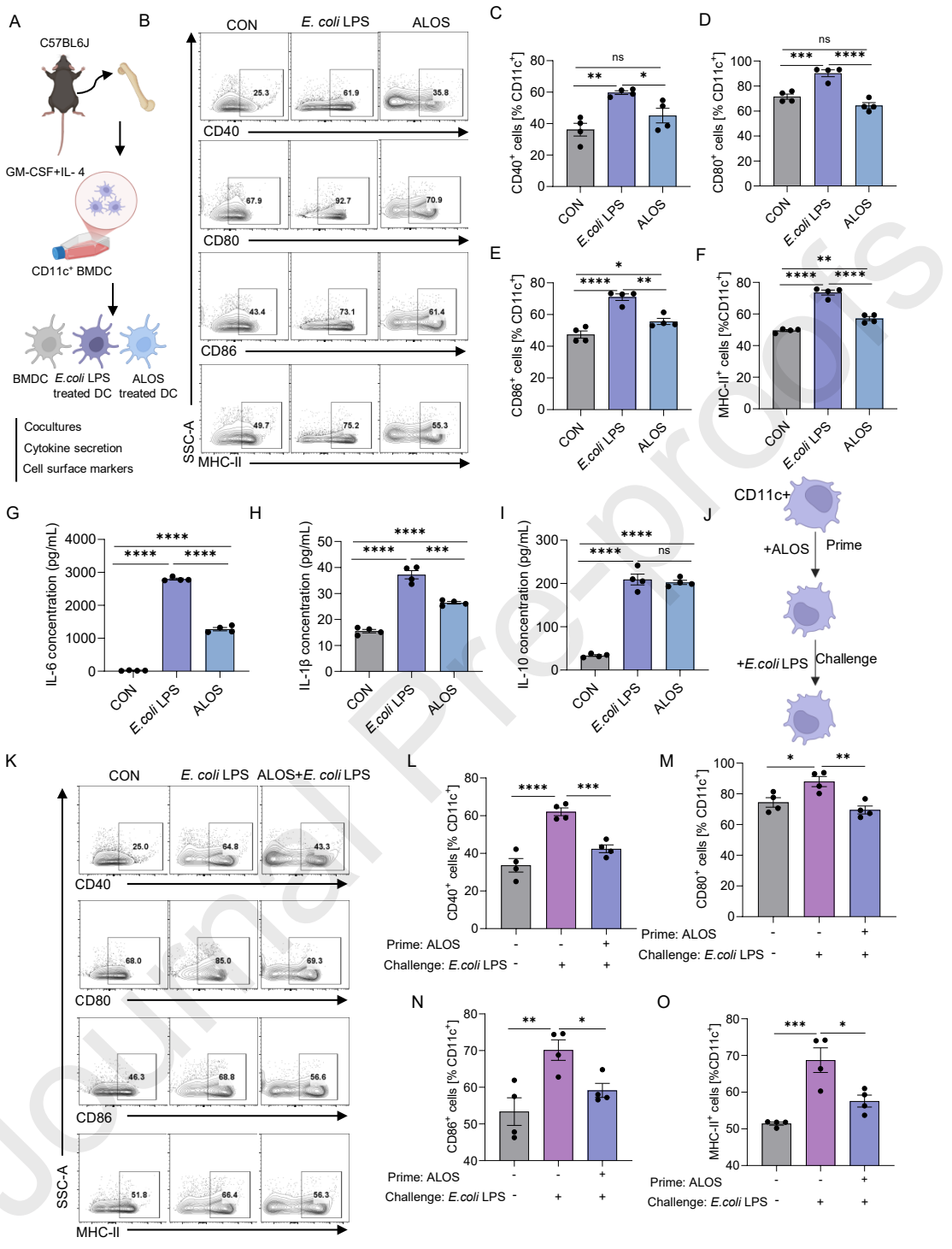

Fig. 4. ALOS induces semi-mature and hyporesponsive dendritic cells (DCs). (A) Schematic of the *in vitro* stimulation of WT BMDCs. Cells were treated with PBS (control BMDC),100ng/mL *E. coli* LPS (positive control, *E. coli* LPS), 100ng/mL ALOS (experimental, ALOS) for 12h. (B) Gating strategy of flow analysis to examine surface expressions of MHC class II, CD40, CD80, and CD86 in BMDCs. (C-F) The population of $CD40^{+}$DC(C), $CD80^{+}$ DC (D), $CD86^{+}$ DC (E), and MHC class II^{+} DCs(F).

(G-I) The concentration of cytokines IL-6(G), IL-1β(H), IL-10(I) in cell-free supernatant of BMDCs. (J) Schematic of the two-step *in vitro* stimulation protocol. WT BMDCs were stimulated with 100ng/mL ALOS for 12h (prime). After replacing the medium, cells were challenged with *E. coli* LPS (challenge) for an additional 6 h. (K) Surface expressions of CD40, CD80, CD86 and MHC class II in BMDCs, were detected by flow cytometry. (L-O) The population of $CD40^{+}$DC(L), $CD80^{+}$DC(M), $CD80^{+}$DC(N), and MHC class II^{+} DCs(O). *p<0.05, **p<0.01, ***p<0.001, ****p<0.0001, ns p>0.05 (One-way ANOVA in C-I, L-O. Results were expressed as the mean ± SEM). n values: (C-I, L-O) n=4.

Figure 5

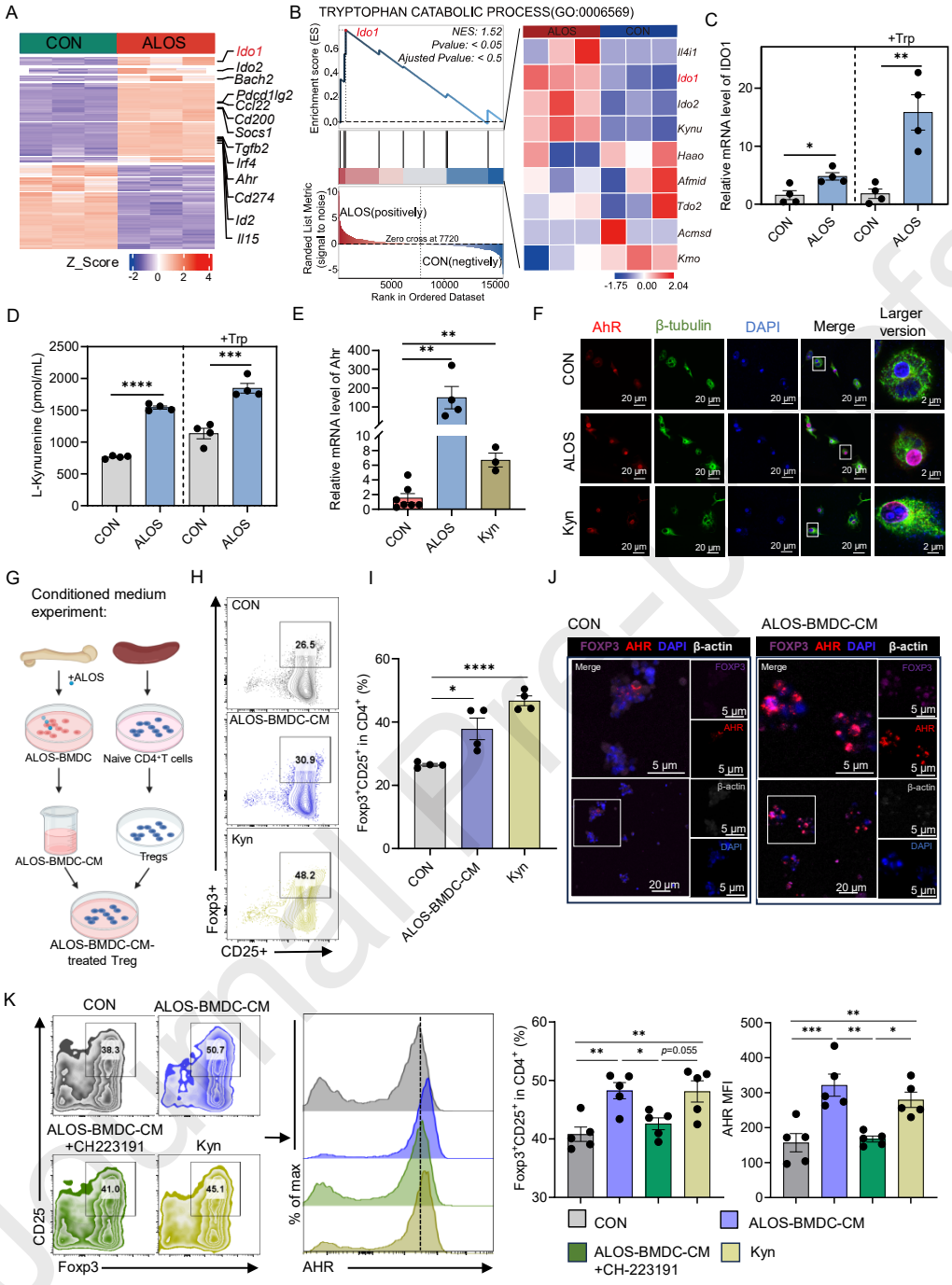

Fig. 5. ALOS activates the IDO1-Kyn-AhR axis. (A) Heatmap of representative differentially expressed genes in the BMDCs showing significant changes between the CON group and the ALOS treatment group. Colors indicate expression changes of genes, with red denoting increased and blue decreased levels. Data represent the means of normalized maximum intensities, then Z-score transformed and displayed as heatmaps. (B) Gene Set Enrichment Analysis (GSEA) of Tryptophan catabolic process. (C) Genes expression of IDO1 in BMDCs under basal conditions and in response to tryptophan (Trp) supplementation. (D) The production of Kynurenine (Kyn) in BMDCs

under basal conditions and in response to tryptophan (Trp) supplementation. (E) mRNA expression levels of AhR between the CON group and the ALOS treated BMDCs. (F) Immunofluorescence staining of AhR in BMDC. (G) Schematic of the experimental design to assess the effect of conditioned medium from ALOS-BMDCs on Treg cells. (H) Flow cytometry analysis of $Foxp3^+$ $CD25^+$ CD4 T cells under the conditions of ALOS-BMDC conditioned medium or Kyn. (I) The proportion of Tregs under the conditions of ALOS-BMDC conditioned medium or Kyn. (J) Immunofluorescence staining of Foxp3 and AhR in induced-Treg cells. (K) The proportion of Tregs and the expression of AhR on Tregs under the conditions of ALOS-BMDC-CM, ALOS-BMDC-CM+CH-223191, Kyn. Differentially expressed genes between untreated and ALOS-treated BMDCs were identified using the following criteria: $|\log_2 \text{fold change}| > 1$ and adjusted p-value < 0.05. Multiple testing correction was performed using the Benjamini–Hochberg method to control the false discovery rate. *p<0.05, **p<0.01, ***p<0.001, ****p<0.0001, ns p>0.05 (Unpaired two- tailed Student's t- test in C–E; One-way ANOVA in I, K. Results were expressed as the mean ± SEM). n values: (A, B) n=3, (C-F, H, I) n=4, (K) n=5.

Figure 6

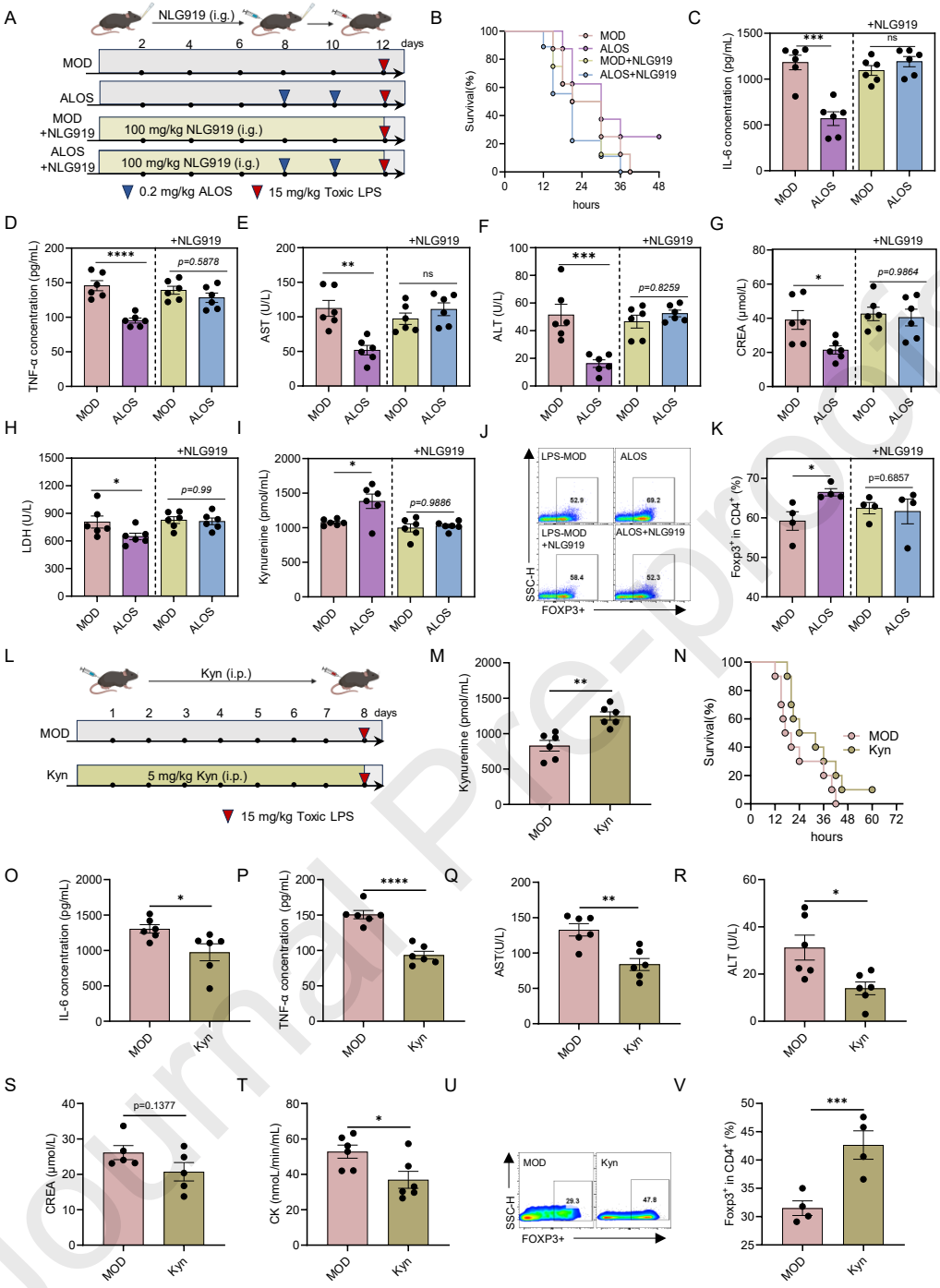

Fig. 6. The anti-sepsis effect of ALOS requires activation of IDO1. (A) Schematic diagram for the several treatment groups. The diagram illustrates the following interventions: Control MOD (15mg/kg *Escherichia coli* LPS). NLG919 (Navoximod), an IDO1 inhibitor. (B) Survival rate. (C-I) The plasma concentrations of IL-6(C), TNF-α(D), AST(E), ALT(F), CREA(G), LDH(H), Kyn(I). (J-K) The proportion of Tregs (Foxp3$^+$ CD4 T cells) were detected by flow cytometry. (L) Experimental design illustrating the effect of Kyn. (M) The levels of Kyn. (N) Survival rate. (O-T) The plasma concentrations of IL-6(O), TNF-α(P), AST(Q), ALT(R), CREA(S), CK(T). (U-V) The proportion of Tregs (Foxp3$^+$ CD4 T cells) on Tregs were detected by flow

cytometry. *p<0.05, **p<0.01, ***p<0.001, ****p<0.0001, ns p>0.05 (unpaired two-tailed Student's t- test in C-G, M, O-T, V; Mann–Whitney U test in K Results were expressed as the mean ± SEM). n values: (J, K, U, V) n=4, (S) n=5, (C-I, M, O-R, T) n=6, (B) n=8, (N) n=10.

Figure 7

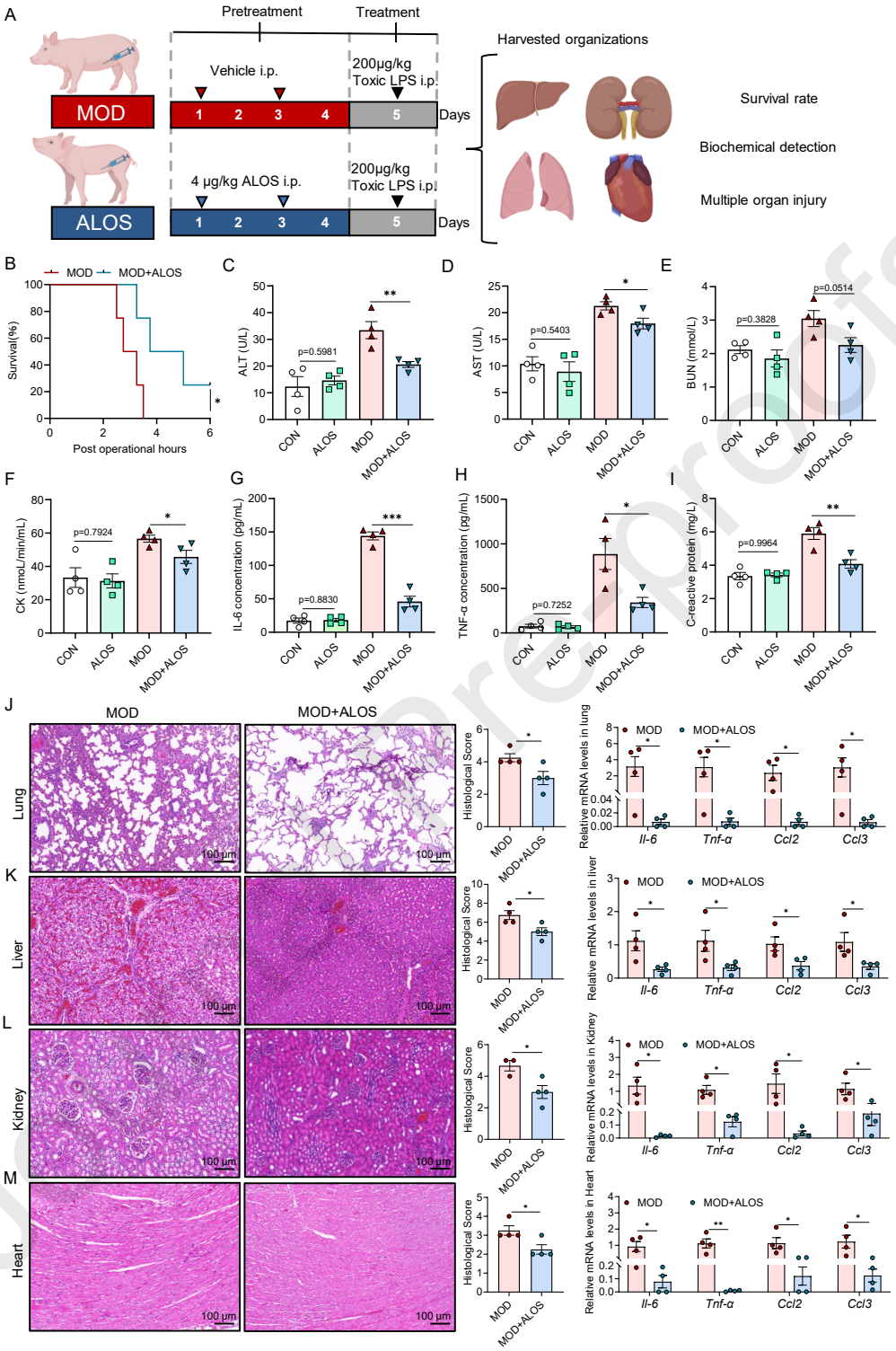

Fig. 7. ALOS mitigates sepsis in a porcine model. (A) Schematic experiment timeline. Piglets were injected with 4 ug/kg ALOS or vehicle before Toxic LPS (200 μg/kg) injection. (B) The survival rates were determined using Kaplan- Meier curve. (C-I) The serum levels of ALT(C), AST(D), blood urea nitrogen (BUN)(E), creatine kinase (CK)(F), IL-6(G), TNF-α(H), C-reactive protein(I) were detected after LPS injection in

piglets pretreated with the vehicle and ALOS. (J-M) Representative H&E staining sections, the histological score and mRNA levels of proinflammatory cytokines of (J) lungs, (K) livers, (L) kidneys, and (M) hearts in piglets pretreated with the vehicle and ALOS (scale bar: 100 μm).*p<0.05; ns p>0.05 (Mantel-Cox log- rank test in B; unpaired two- tailed Student's t- test in C–J. Results were expressed as the mean±SEM). n values: (B-M) n=4.

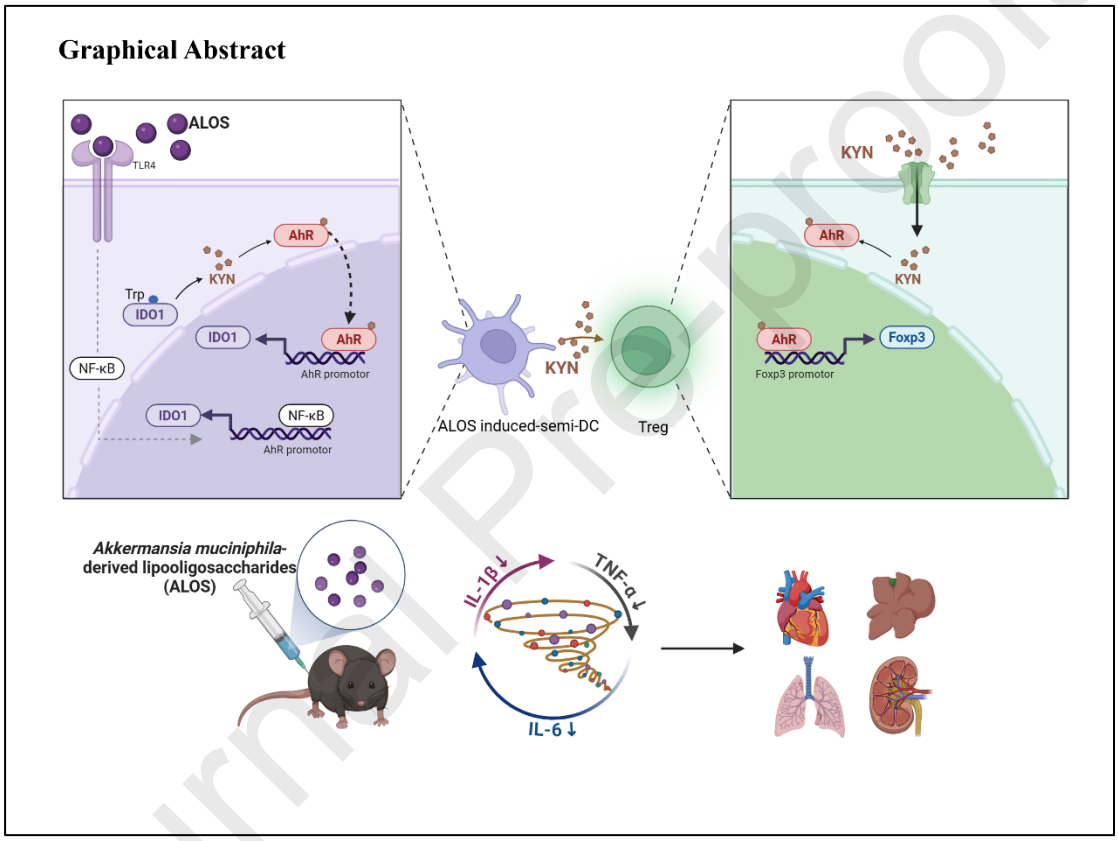

This study reveals that *Akkermansia muciniphila*-derived lipooligosaccharides (ALOS) protect against sepsis by reprogramming immune balance. Mechanistically, ALOS induces semi-mature dendritic cells to activate the IDO1–Kyn–AhR axis, thereby driving Treg differentiation. Validated in both murine and porcine models, this work establishes ALOS as a promising postbiotic therapeutic and elucidates its underlying immunometabolic mechanism.

Research Highlights

This study revealed that the hypoacylated lipooligosaccharides (ALOS) from *Akkermansia muciniphila*, an immunomodulatory postbiotic, significantly improved survival rates and alleviated multi-organ damage in murine models of sepsis induced by lipopolysaccharide and cecal ligation and puncture. Its systemic anti-inflammatory and organ-protective effects were also verified in a porcine sepsis model, demonstrating its transformation potential.

ALOS enhanced ILC3-derived IL-22 expression, promoted intestinal stem cell markers, tight junction proteins, and upregulated antimicrobial peptides Reg3g and Reg3b. It reshaped the gut microbiota by enriching *Dubosiella* sp00403415 and *Lactobacillus johnsonii*, thereby establishing a gut microbiota benefiting for resisting inflammatory diseases.

ALOS can systematically restore the immune imbalance state of sepsis mouse, shifting macrophages from an inflammatory phenotype ($CD86^+$) to an anti-inflammatory phenotype ($CD206^+$), significantly reducing the proportion of pro-inflammatory Th17 cells and increasing the number of anti-inflammatory Treg cells, thereby restoring the Th17/Treg immune balance.

Mechanistically, ALOS induced semi-mature dendritic cells, upregulated the key immune tolerance enzyme IDO1 to promot kynurenine (Kyn) production, which activated the aryl hydrocarbon receptor (AhR) and drived regulatory T cell (Treg) differentiation, thereby establishing the IDO1-Kyn-AhR immunoregulatory axis.

Graphical Abstract

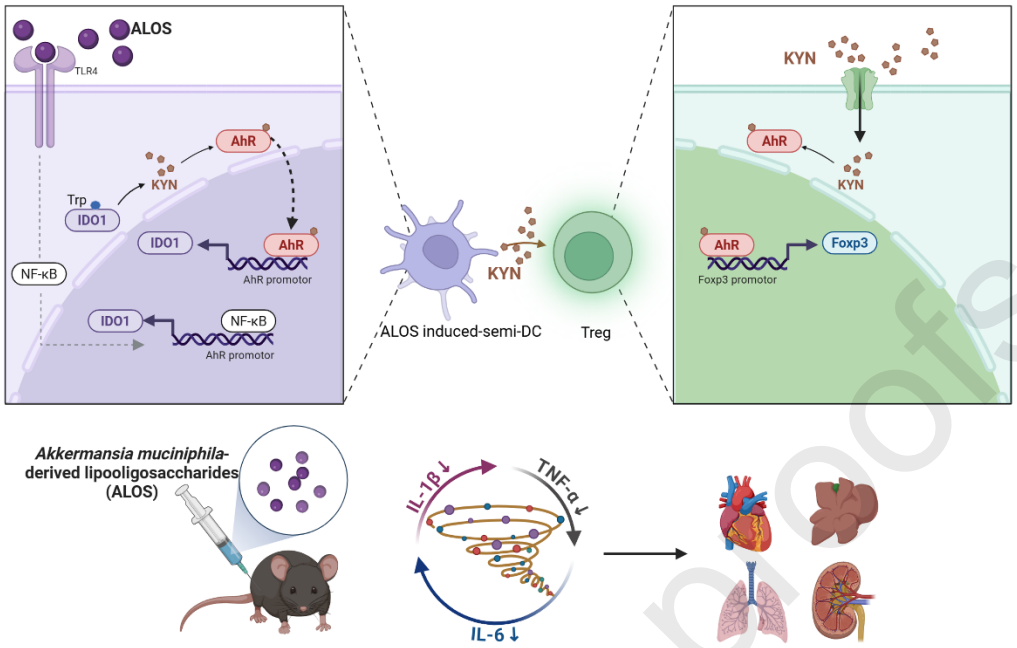

Conflict of Interest

The authors have declared no conflict of interest

Corresponding author

Name: (刘宏伟)

Affiliation: State Key Laboratory of Microbial Diversity and Innovative Utilization, Institute of Microbiology, Chinese Academy of Sciences, Beijing, P. R. China.
Tel./ Mobile Number: +86（10）64806074

E-mail address: liuhw@im.ac.cn